

Study of Neutrino Phenomenology and $0\nu\beta\beta$ Decay using Polyharmonic $Maa\beta$ Forms

Bhabana Kumar^{1,*} and Mrinal Kumar Das^{1,†}

¹*Department of Physics, Tezpur University, Tezpur 784028, India*

Abstract

In this study, we explore the application of the Γ_3 modular group, which is isomorphic to the A_4 symmetric group in developing a model for neutrino mass. We realized a non-supersymmetric left-right asymmetric model incorporating modular symmetry, where the modular forms consist of both holomorphic and non-holomorphic components and the Yukawa couplings expressed through polyharmonic $Maa\beta$ forms. To effectively implement the extended see-saw process in this model, we introduce one fermion singlet for each generation. We compute the effective mass and the associated half-life of $0\nu\beta\beta$ by accounting for both standard and non-standard contributions. Additionally, our study investigates the non-unitary effects and CP-violation arising from non-unitarity in this context. The model predicts values for the sum of neutrino masses and neutrino oscillation parameters are consistent with experiments. Furthermore, it yields satisfactory results in calculating the effective mass and half-life of $0\nu\beta\beta$ decay. These findings highlight the possibility and benefit of employing modular symmetry in neutrino mass model construction.

arXiv:2405.10586v3 [hep-ph] 22 Jul 2025

* bhabana12@tezu.ernet.in

† mkdas@tezu.ernet.in

I. INTRODUCTION

One of the most recognized and thoroughly tested particle physics models to date is the Standard Model (SM). In addition to explaining interactions between all of the known fundamental particles, SM also describes their properties, such as mass, charge, spin, and so forth. Despite being successful, SM is not without limitations. One significant drawback is its inability to account for the tiny neutrino masses. Except for the neutrino, every fermion in the context of SM is massive, and the Higgs mechanism gives those fermions their mass. The Higgs mechanism requires both the left and right-handed counter particles to couple with the Higgs field for a particle to gain mass. However, due to the lack of right-handed counter particles of neutrinos, it is not possible to incorporate massive neutrinos within the framework of SM. The idea of a massless neutrino is completely denied by the discovery of neutrino oscillation. Experiments like Superkamiokande [1] and SNO [2–4] have provided strong evidence for neutrino oscillation, a phenomenon that is not possible if the neutrino is massless. To learn more about neutrinos, several experiments, including MINOS [5], Daya-Bay [6], TK2 [7], RENO [8], and others, have been carried out, and all those experiments have suggested non-zero and non-degenerate neutrino masses. Neutrino oscillation experiments have played a crucial role in refining our knowledge of neutrinos and providing insights into their properties. Scientists have been able to determine the mass squared differences and mixing angles associated with neutrinos. While substantial progress has been made in determining the oscillation parameters, there is still much we do not know definitively about neutrinos. The Planck experiment recently provided an approximate upper bound on the sum of the neutrino masses, which is equal to $\sum m_\nu = 0.11$ eV [9]. However, the exact masses of neutrino and their mass hierarchy [10, 11] remain unclear. Additionally, the nature of neutrinos, whether they are Dirac or Majorana particles [12, 13], is still a subject of ongoing study.

The limitations of the SM extend beyond neutrino masses. It fails to explain origin of CP violation in weak interactions, lepton flavor violation, the baryon asymmetry of the universe, dark matter, and dark energy. To address these shortcomings, we need to go beyond the SM and explore extensions that involve the addition of new fermion or scalar particles. The seesaw mechanism is a prominent extension that offers explanations to the tiny neutrino mass problem. There are different types of seesaw mechanisms, such as Type I [14–16], Type II [17–19], and Type III [20]. In these models, the SM is extended by incorporating right-handed neutrinos, $SU(2)_L$ scalar triplet, or $SU(2)_L$ triplet fermion, respectively, to generate small but nonzero neutrino masses.

Another beyond SM framework is the Left-Right symmetric model (LRSM) [21–24], which extends the SM by introducing additional gauge symmetries. The gauge group of the LRSM is $SU(3)_C \times SU(2)_L \times SU(2)_R \times U(1)_{B-L} \times D(G_{221D})$. This model has gained significant attention in the literature due to its success in explaining the tiny neutrino masses observed experimentally as well as addressing other

drawbacks of the SM. Even though the model is very successful in many aspects, ambiguity arises when one wants to incorporate the LRSM within the Grand Unified Theory (GUT). To embed LRSM within GUT like $SO(10)$, requires the parity breaking scale to be very high, only then one will get the observed value of $\sin^2 \theta_W$ [25], but in LRSM both the D-parity and $SU(2)_R$ gauge groups break at the same energy scale, which implies that all the phenomena involving right-handed current will get highly suppressed under this condition. However, an alternative approach to the LRSM is the left-right asymmetric model [26, 27], where the D-parity is decoupled from the $SU(2)_R$ gauge group at a very high energy scale. This decoupling results in different gauge coupling values for the $SU(2)_L$ and $SU(2)_R$ gauge groups, leading to an asymmetry in the model. In this left-right asymmetric model, the gauge coupling value of $SU(2)_L$ is not equal to the gauge coupling value of $SU(2)_R$, that is, $g_l \neq g_r$. This alternative approach is intriguing because the different gauge coupling values can either suppress or enhance various low-energy phenomena, offering unique predictions.

For many years discrete symmetry groups like A_4 , S_4 , S_3 have been used for model building purposes in the lepton sector [28–34]. But one of the main disadvantages is the requirement of "flavon" to spontaneously break such symmetry and the vacuum expectation value (V.E.V) of such field can significantly affect the physical prediction of the model. In recent years, the application of modular symmetry in particle physics has received significant attention due to its ability to explain the patterns and hierarchies observed in fermions, also modular symmetry gained its popularity because one can construct a model without using any "flavon" since in modular symmetry modulus τ is responsible for breaking the flavor symmetry [35–38]. Many research groups have been working on model building by using modular group like Γ_3 [39–46], Γ_4 [47–50], Γ_5 [51] etc.

In our current work, we have focused on studying neutrino masses and mixing within the left-right asymmetric model. So far, model building using modular symmetry has been done in the framework of supersymmetry due to the holomorphic nature of modular forms [38]. However, in our case, we are working in a non-supersymmetric framework inspired by automorphic forms [52, 53]. Here, the concept of holomorphicity is replaced by the Laplacian condition, where holomorphicity is substituted with the harmonic condition and the Yukawa couplings are polyharmonic $Maa\beta$ forms of level N , which can be arranged into multiplets of the finite modular groups Γ_N and Γ'_N . The level N polyharmonic $Maa\beta$ forms match the level N holomorphic modular forms at weights $k \geq 3$. However, this framework allows for the existence of polyharmonic $Maa\beta$ forms with negative and zero weights. In the case of Γ_3 modular group, which is isomorphic to A_4 group, for $k \leq 2$, we always have four polyharmonic $Maa\beta$ forms among which one is a singlet and the other three forming a triplet of A_4 . So in the present work, we have used the idea of automorphic forms, and we have studied neutrinoless double beta ($0\nu\beta\beta$) decay within this framework. By utilizing this mathematical framework, we have derived mass matrices that govern the neutrino sector of the model and implemented those matrices to calculate and study neutrino

masses, effective neutrino mass, and half-life of $0\nu\beta\beta$ decay.

The overall structure of the paper is as follows: In Section II, we provide a brief introduction to the left-right asymmetric model. In Section III, we present an overview of modular symmetry. In Section IV, we thoroughly discuss the model. In Section V, we provide an overview of the extended inverse seesaw mechanism, while in Section VI, we discuss the unitary violation in the lepton sector. In Section VII, we examine the contribution to $0\nu\beta\beta$ decay. A detailed discussion of the numerical analysis and results of our study is presented in Section VIII. Finally, we summarize our findings in Section IX.

II. LEFT-RIGHT ASYMMETRIC MODEL

The initial proposal of the left-right asymmetry model was put forth by Chang, Mohapatra, and Parida in their publication [54]. An alternate method has been proposed to decouple D-parity from the $SU(2)_R$ gauge group at high energy scales while preserving the original gauge symmetry [26, 27]. The decoupling of D-parity from the $SU(2)_R$ gauge group occurs when the odd parity singlet scalar field η , acquires a vacuum expectation value (V.E.V) at an energy scale denoted as M_P . The outcome is an asymmetrical left-right model in which the gauge couplings of $SU(2)_L$ and $SU(2)_R$ becomes unequal, i.e., $g_l \neq g_r$. The entire symmetry-breaking steps can be illustrated as follows :

$$\begin{aligned}
& SU(2)_L \times SU(2)_R \times U(1)_{B-L} \times SU(3)_C \times D \\
& \quad \downarrow \quad \eta \\
& SU(2)_L \times SU(2)_R \times U(1)_{B-L} \times SU(3)_C \\
& \quad \downarrow \Sigma \\
& SU(2)_L \times U(1)_R \times U(1)_{B-L} \times SU(3)_C \\
& \quad \downarrow \Delta_R \\
& SU(2)_L \times U(1)_Y \times SU(3)_C \\
& \quad \downarrow \quad \Phi \\
& U(1)_{em} \times SU(3)_C.
\end{aligned}$$

After the spontaneous breaking of D-parity, the asymmetric gauge group undergoes two possible paths. The first path occurs when the Higgs triplet Δ_R gains a non-zero vacuum expectation value, leading to the breakdown of the left-right asymmetric model into SM gauge group. Subsequently, the SM gauge group further breaks down to $U(1)_{em}$ when both the left-handed Higgs triplet and the bidoublet acquire non-zero V.E.V.

On the other hand, in the alternative path, the gauge group $SU(2)_R$ initially breaks down to $U(1)_R$ when a heavier scalar triplet, $\Sigma(1, 3, 0)$, carrying $B - L = 0$, obtains a non-zero V.E.V. This step of

symmetry breaking leads to the generation of massive W_R^\pm gauge bosons. Finally, in the last step, the intermediate gauge group $U(1)_R \times U(1)_{B-L}$ breaks down to SM gauge group when either a doublet, a triplet, or both the doublet and triplet gain non-zero V.E.V [55]. During this step, the right-handed neutral gauge boson Z_R^0 obtains its mass. The minimal particle content of the model and their charge assignments under the gauge group G_{221} are given below

$$Q_L = \begin{pmatrix} u_L \\ d_L \end{pmatrix}, \quad Q_R = \begin{pmatrix} u_R \\ d_R \end{pmatrix}, \quad \Psi_L = \begin{pmatrix} \nu_L \\ l_L \end{pmatrix}, \quad \Psi_R = \begin{pmatrix} \nu_R \\ l_R \end{pmatrix}$$

$$Q_L : (2, 1, 1/3) \quad Q_R : (1, 2, 1/3) \quad \Psi_L : (2, 1, -1) \quad \Psi_R : (1, 2, -1)$$

and the required Higgs multiplets are

$$\phi = \begin{pmatrix} \phi_1^0 & \phi_1^+ \\ \phi_2^- & \phi_2^0 \end{pmatrix}, \quad \Delta_{L,R} = \begin{pmatrix} \frac{\delta_{L,R}^+}{\sqrt{2}} & \delta_{L,R}^{++} \\ \delta_{L,R}^0 & -\frac{\delta_{L,R}^+}{\sqrt{2}} \end{pmatrix}$$

$$\eta(1, 1, 0), \quad \Phi(2, 2, 0), \quad \Delta_L(3, 1, +2) + \Delta_R(1, 3, +2) .$$

The transformation properties of those scalar field under parity are given below

$$\Delta_L \rightarrow \Delta_R; \quad \Phi \rightarrow \Phi^\dagger; \quad \eta \rightarrow -\eta$$

We can write the individual potential term as follows [54]

$$\begin{aligned} V_\Delta &= \mu_\Delta^2 [Tr(\Delta_L^\dagger \Delta_L) + Tr(\Delta_R^\dagger \Delta_R)] \\ V_\eta &= -\mu_\eta^2 \eta^2 + \lambda \eta^4 \\ V_{\eta\Delta} &= M\eta [Tr(\Delta_L^\dagger \Delta_L) - Tr(\Delta_R^\dagger \Delta_R)] + \lambda_1 \eta^2 [Tr(\Delta_L^\dagger \Delta_L) + Tr(\Delta_R^\dagger \Delta_R)] \\ V_{\eta\Phi} &= \lambda_2 \eta^2 Tr(\phi^\dagger \phi) + \lambda_3 \eta^2 (det\Phi + det\Phi^\dagger) \\ V_{\Delta\Phi} &= \lambda_5 [Tr(\tilde{\Phi})\Delta_R\Phi^\dagger\Delta_L^\dagger + Tr(\tilde{\Phi}^\dagger\Delta_L\Phi\Delta_R^\dagger)] \\ V_\Phi &= \mu_1^2 Tr(\Phi^\dagger\Phi) + \mu_2^2 [Tr(\tilde{\Phi}^\dagger\Phi) + Tr(\tilde{\Phi}\Phi^\dagger)] \end{aligned}$$

After the spontaneous symmetry breaking we can choose the V.E.V of $\Delta_{L,R}$ and Φ as follows

$$\langle \Delta_{L,R} \rangle = \frac{1}{\sqrt{2}} \begin{pmatrix} 0 & 0 \\ \nu_{L,R} & 0 \end{pmatrix}, \quad \langle \Phi \rangle = \begin{pmatrix} k & 0 \\ 0 & \exp(i\phi)k' \end{pmatrix}$$

and the D-parity is broken by $\langle \eta \rangle = \frac{\mu}{\sqrt{2}\lambda}$, which then makes the Δ_L and Δ_R mass terms asymmetric.

III. MODULAR GROUP

The modular group $SL(2, Z) = \Gamma$ is defined as a group of 2×2 matrices with positive or negative integer element and determinant equal to 1 and it represents the symmetry of a torus [37, 56]. It is infinite group and generated by two generators of the group S and T .

$$\Gamma = \left\{ \begin{pmatrix} a & b \\ c & d \end{pmatrix} \mid a, b, c, d \in \mathbb{Z}, ad - bc = 1 \right\} . \quad (3.1)$$

The generator of the group satisfy the conditions:

$$S^2 = 1 \quad \text{and} \quad (ST)^3 = 1$$

and they can be represented by 2×2 matrices

$$S = \begin{pmatrix} 0 & 1 \\ -1 & 0 \end{pmatrix}, \quad T = \begin{pmatrix} 1 & 1 \\ 0 & 1 \end{pmatrix} .$$

A two-dimensional space is obtained, when the torus is cut open and this two-dimensional space can be viewed as an Argand plane and modulus τ is the lattice vector of that Argand plane. The transformation of modulus τ [57] of the modular group on the upper half of the complex plane is given below

$$\gamma : \tau \rightarrow \gamma(\tau) = \frac{(a\tau + b)}{(c\tau + d)}$$

the transformation of τ is same for both γ and $-\gamma$ and we can define a group $\bar{\Gamma} = PSL(2, Z)$, which is a projective special linear group. Also, the modular group has an infinite number of normal subgroups, which is the principal congruence subgroup of level N and can be defined as

$$\Gamma(N) = \left\{ \begin{pmatrix} a & b \\ c & d \end{pmatrix} \in SL(2, Z), \begin{pmatrix} a & b \\ c & d \end{pmatrix} = \begin{pmatrix} 1 & 0 \\ 0 & 1 \end{pmatrix} \pmod{N} \right\}, \quad (3.2)$$

and for $N > 2$, $\bar{\Gamma}(N) = \Gamma_N$. The use of a finite group is essential for the purposes of model building. Usually a modular group is an infinite group but we can obtain a finite modular group for $N > 2$, if we consider the quotient group $\Gamma_N = PSL(2, Z)/\bar{\Gamma}(N)$ and these modular group are isomorphic to non-abelian discrete groups. The modular invariance requires the Yukawa couplings to be a certain modular function $Y(\tau)$ and should follow the following transformation property.

$$Y(\gamma\tau) = (c\tau + d)^k Y(\tau) \quad (3.3)$$

So far modular symmetry has been used in the context of supersymmetry where the superpotential is the holomorphic function of modulus τ . However, some recent works have been developed where we can use modular symmetry to develop the non-supersymmetric model. The basic idea is that one can realise the non-supersymmetric framework by using the framework of automorphic forms and the assumption of

holomorphicity is replaced by the Laplacian condition. In such case the Yukawa coupling can have both holomorphic and non-holomorphic parts [52, 53, 58]. In the present work, we are concerned with the polyharmonic $Maa\beta$ forms of weight k and the Yukawa coupling needs to follow another transformation property, which is given below

$$\Delta_k Y(\tau) = 0 \quad (3.4)$$

where $\tau = x + iy$ and Δ_k is the hyperbolic Laplacian operator

$$\Delta_k = -y^2 \left(\frac{\partial^2}{\partial x^2} + \frac{\partial^2}{\partial y^2} \right) + iky \left(\frac{\partial}{\partial x} + i \frac{\partial}{\partial y} \right) = -4y^2 \frac{\partial}{\partial \tau} \frac{\partial}{\partial \bar{\tau}} + 2iky \frac{\partial}{\partial \tau} \quad (3.5)$$

The weight k of polyharmonic $Maa\beta$ forms can be positive, zero, or even negative. Based on the transformation property given in the equation (3.3), which implies that $Y(\tau+N) = Y(\tau)$ and considering the transformation property from equation (3.4), the Fourier expansion of a level N and weight k polyharmonic $Maa\beta$ form can be expressed as[52]

$$Y(\tau) = \sum_{n \in \frac{1}{N}\mathbb{Z}, n \geq 0} c^+(n) q^n + c^-(0) y^{1-k} + \sum_{n \in \frac{1}{N}\mathbb{Z}, n < 0} c^-(n) \Gamma(1-k, -4\pi n y) q^n \quad (3.6)$$

where $q = e^{i2\pi\tau}$.

Table I shows the summary of polyharmonic $Maa\beta$ forms of weights $k_Y = -4, -2, 0, 2, 4, 6$ at level $N = 3$ [52].

In the present work, since we are working in the non-supersymmetric framework, we have focused on

Weight k_Y	Polyharmonic $Maa\beta$ forms $Y_r^{k_Y}$
$k_Y = -4$	Y_1^{-4}, Y_3^{-4}
$k_Y = -2$	Y_1^{-2}, Y_3^{-2}
$k_Y = 0$	Y_1^0, Y_3^0
$k_Y = 2$	Y_1^2, Y_3^2
$k_Y = 4$	$Y_1^4, Y_{1'}^4, Y_3^4$
$k_Y = 6$	$Y_1^6, Y_{3I}^6, Y_{3II}^6$

TABLE I: Polyharmonic $Maa\beta$ forms for different weight at level three

polyharmonic $Maa\beta$ forms of weight zero at level 3. It can be arranged into a singlet and triplet under

A_4 group. The q expansion of the weight zero Yukawa couplings at level three is provided below

$$\begin{aligned}
Y_{3,1}^{(0)} &= y - \frac{3e^{-4\pi y}}{\pi q} - \frac{9e^{-8\pi y}}{2\pi q^2} - \frac{-12\pi y}{\pi q^3} - \frac{21e^{-16\pi y}}{4\pi q^4} - \frac{18e^{-20\pi y}}{5\pi q^5} - \frac{3e^{-24\pi y}}{2\pi q^6} + \dots \\
&\quad - \frac{9 \log 3}{4\pi} - \frac{3q}{\pi} - \frac{9q^2}{2\pi} - \frac{q^3}{\pi} - \frac{21q^4}{4\pi} - \frac{18q^5}{5\pi} - \frac{3q^6}{2\pi} \\
Y_{3,2}^{(0)} &= \frac{27q^{\frac{1}{3}}e^{\frac{\pi y}{3}}}{\pi} \left(\frac{e^{-3\pi y}}{4q} + \frac{e^{-7\pi y}}{5q^2} + \frac{5e^{-11\pi y}}{16q^3} + \frac{2e^{-15\pi y}}{11q^4} + \frac{2e^{-19\pi y}}{7q^5} + \frac{4e^{-23\pi y}}{17q^6} + \dots \right) \\
&\quad + \frac{9q^{\frac{1}{3}}}{2\pi} \left(1 + \frac{7q}{4} + \frac{8q^2}{7} + \frac{9q^3}{5} + \frac{14q^4}{13} + \frac{31q^5}{16} + \frac{20q^6}{19} + \dots \right) \\
Y_{3,3}^{(0)} &= \frac{9q^{\frac{2}{3}}e^{\frac{2\pi y}{3}}}{2\pi} \left(\frac{e^{-2\pi y}}{q} + \frac{7e^{-6\pi y}}{4q^2} + \frac{8e^{-10\pi y}}{7q^3} + \frac{9e^{-14\pi y}}{5q^4} + \frac{14e^{-18\pi y}}{13q^5} + \frac{31e^{-22\pi y}}{16q^6} + \dots \right) \\
&\quad + \frac{27q^{\frac{2}{3}}}{\pi} \left(\frac{1}{4} + \frac{q}{5} + \frac{5q^2}{16} + \frac{2q^3}{11} + \frac{2q^4}{7} + \frac{9q^5}{17} + \frac{21q^6}{20} + \dots \right)
\end{aligned} \tag{3.7}$$

A_4 is a finite modular group and isomorphic to Γ_3 group. A_4 group is a non-Abelian discrete group and has a total of four irreducible representations, among which three are one-dimensional and one is three-dimensional. A brief introduction about the A_4 group is given in the Appendix C.

IV. THE MODEL

To implement Γ_3 modular group, we have considered the intermediate asymmetric gauge group $SU(2)_L \times U(1)_R \times U(1)_{B-L} \times SU(3)_C$ and have used the scalar triplet (Δ_R) and doublet (χ_R) to break the intermediate asymmetric group to the SM gauge group. We have considered an extra sterile fermion per generation to generate the light neutrino mass via extended inverse seesaw mechanism [59–61]. The Yukawa Lagrangian term associated with the model is given in equation 4.1

$$\mathcal{L} = \mathcal{L}_l + \mathcal{L}_D + \mathcal{L}_M + \mathcal{L}_{N-S} + \mathcal{L}_S + h.c. \quad . \tag{4.1}$$

Where \mathcal{L}_l is the Yukawa Lagrangian term for the charged lepton, \mathcal{L}_D is the Dirac Yukawa Lagrangian term for the neutral lepton, \mathcal{L}_M and \mathcal{L}_{N-S} are the Majorana and neutrino-sterile (N-S) mixing terms respectively and finally \mathcal{L}_S is the self-coupling term for the sterile fermion. In Table II we have provided the charge assignments and modular weights for the particle contents of the model. The charge assignment under $U(1)_R$ corresponds to the third or z-component of isospin i.e., T_{3R} of $SU(2)_R$ and the equation $Q = T_{3L} + T_{3R} + \frac{B-L}{2}$ is also valid for the gauge group G_{2113} .

A. Mass term for charged leptons

To construct a diagonal charged lepton mass matrix, we consider the three-generation left-handed lepton doublet $\Psi_{L_i} (i = 1, 2, 3)$ transforming as $1, 1', 1''$ under the A_4 group. Similarly, the three

Field	Ψ_{R_i}	Ψ_{L_i}	N_R	S	Φ	Δ_R	χ_R
$SU(2)_L$	1	2	1	1	2	1	1
$U(1)_R$	$-\frac{1}{2}$	0	$\frac{1}{2}$	0	$-\frac{1}{2}$	-1	$\frac{1}{2}$
A_4	$1, 1'', 1'$	$1, 1', 1''$	3	3	1	1	1
k_I	0	0	0	0	0	0	0

TABLE II: Charge assignment for the particle content of the model

right-handed charged leptons $\Psi_{R_i} (i = 1, 2, 3)$ transform as $1, 1'', 1'$ under the A_4 group. The Yukawa Lagrangian term for the charged leptons and the corresponding diagonal charged lepton mass matrix are given in equations (4.2) and (4.3), respectively.

$$\mathcal{L}_l = \alpha \Phi \bar{\Psi}_{L_1} Y_1^0 \Psi_{R_1} + \beta \Phi \bar{\Psi}_{L_2} Y_1^0 \Psi_{R_2} + \gamma \Phi \bar{\Psi}_{L_3} Y_1^0 \Psi_{R_3} \quad (4.2)$$

The modular form Y_1^0 is a constant, while α, β , and γ are adjustable parameters. By choosing appropriate values for these parameters, we obtain the desired charged lepton mass matrix.

$$M_D = v \begin{pmatrix} Y_1^0 \alpha & 0 & 0 \\ 0 & Y_1^0 \beta & 0 \\ 0 & 0 & Y_1^0 \gamma \end{pmatrix}. \quad (4.3)$$

B. Dirac mass term for neutrino

To construct the A_4 invariant Dirac mass term, we assume that the lepton doublets Ψ_{L_i} transform as $1, 1', 1''$, while the right-handed neutrinos N_R transform as triplets, and the Higgs bidoublet transforms as a singlet under the A_4 group. The corresponding A_4 invariant Dirac Yukawa interaction is given in (4.4).

$$\mathcal{L}_D = g_1 \Phi \bar{\Psi}_{L_1} (Y_3^{(0)} N_R)_1 + g_2 \Phi \bar{\Psi}_{L_2} (Y_3^{(0)} N_R)_{1''} + g_3 \Phi \bar{\Psi}_{L_3} (Y_3^{(0)} N_R)_{1'} \quad (4.4)$$

Where g_1, g_2 and g_3 are adjustable parameters of the model. From equation (4.4), we can construct the Dirac mass matrix of the model, which is given in equation (4.5)

$$M_D = v \begin{pmatrix} g_1 Y_{3,1}^{(0)} & g_1 Y_{3,3}^{(0)} & g_1 Y_{3,2}^{(0)} \\ g_2 Y_{3,3}^{(0)} & g_2 Y_{3,2}^{(0)} & g_2 Y_{3,1}^{(0)} \\ g_3 Y_{3,2}^{(0)} & g_3 Y_{3,1}^{(0)} & g_3 Y_{3,3}^{(0)} \end{pmatrix}. \quad (4.5)$$

Where $v = 246$ GeV is the V.E.V of the bidoublet Φ , and (g_1, g_2, g_3) are adjustable complex parameters of the model. Their values are chosen such that all the neutrino oscillation parameters fall within the 3σ range and the real and imaginary parts of those free parameters lie within the range of 0.4 to 0.8.

C. Majorana mass term for neutrino

We have assigned a singlet to the scalar triplet Δ_R , and by considering the symmetric nature of the Majorana mass term we can write the Majorana mass term, in the following way:

$$\mathcal{L}_{M_R} = g_4 \Delta_R Y_3^{(0)} (\bar{N}^C_R N_R)_{3_S} + g_5 \Delta_R Y_1^{(0)} (\bar{N}^C_R N_R)_1 \quad . \quad (4.6)$$

From equation (4.6), we have constructed the Majorana mass matrix. In equation (4.7), v_R is the V.E.V of the scalar triplet Δ_R , and is taken to be 3 TeV in our analysis. g_4 and g_5 are complex adjustable parameters of the model and we have chosen their real and imaginary parts to lie within the range of 0.4 to 0.8.

$$M = v_R \begin{pmatrix} g_5 + 2g_4 Y_{3,1}^{(0)} & -g_4 Y_{3,3}^{(0)} & -g_4 Y_{3,2}^{(0)} \\ -g_4 Y_{3,3}^{(0)} & 2g_4 Y_{3,2}^{(0)} & g_5 - g_4 Y_{3,1}^{(0)} \\ -g_4 Y_{3,2}^{(0)} & g_5 - g_4 Y_{3,1}^{(0)} & 2g_4 Y_{3,3}^{(0)} \end{pmatrix} \quad (4.7)$$

D. N-S mixing term

The sterile fermion S_i ($i = 1, 2, 3$) and the scalar doublet χ_R both transform as singlets under the A_4 group, and the scalar doublet χ_R is responsible for $N - S$ mixing. The A_4 invariant $N - S$ mixing term is given in the equation (4.8)

$$\mathcal{L}_N = f_1 \chi_R (\bar{N}_R S)_{3_S} Y_3^{(0)} + f_2 \chi_R (\bar{N}_R S)_{3_A} Y_3^{(0)} + f_3 \chi_R (\bar{N}_R S)_1 Y_1^0 \quad . \quad (4.8)$$

Here, f_1 , f_2 and f_3 are complex, adjustable parameters of the model, whose values can be adjusted to achieve the desired results. In the present case, their real and imaginary components are assumed to lie within the range of 0.1 to 1. From the above equation, we have constructed the $N - S$ mixing mass matrix, which is given in equation (4.9)

$$M = v' \begin{pmatrix} f_3 + 2f_1 Y_{3,1}^{(0)} & (-f_1 + f_2) Y_{3,3}^{(0)} & (-f_1 - f_2) Y_{3,2}^{(0)} \\ (-f_1 - f_2) Y_{3,3}^{(0)} & 2f_1 Y_{3,2}^{(0)} & f_3 + (-f_1 + f_2) Y_{3,1}^{(0)} \\ (-f_1 + f_2) Y_{3,2}^{(0)} & f_3 + (-f_1 - f_2) Y_{3,1}^{(0)} & 2f_1 Y_{3,3}^{(0)} \end{pmatrix} \quad . \quad (4.9)$$

The V.E.V associated with the scalar doublet χ_R , represented by v' , is assumed to be 1 TeV in the present analysis.

E. Sterile-Sterile ($S - S$) mixing term

This is the Majorana mass term for the sterile fermion. Equations (4.10) and (4.11), represent the $S - S$ mixing mass term and the corresponding mass matrix, respectively. We have taken g_6 and g_7

within the range of 10 keV to 50 keV.

$$\mathcal{L}_S = g_6(S^T S) + g_7 Y_3^0 (S^T S)_{3_S} . \quad (4.10)$$

$$M_S = \begin{pmatrix} g_6 + 2g_7 Y_{3,1}^{(0)} & -g_7 Y_{3,3}^{(0)} & -g_7 Y_{3,2}^{(0)} \\ -g_7 Y_{3,3}^{(0)} & 2g_7 Y_{3,2}^{(0)} & g_6 - g_7 Y_{3,1}^{(0)} \\ -g_7 Y_{3,2}^{(0)} & g_6 - g_7 Y_{3,1}^{(0)} & 2g_7 Y_{3,3}^{(0)} \end{pmatrix} . \quad (4.11)$$

V. EXTENDED INVERSE SEESAW MECHANISM

Spontaneous symmetry breaking of the Yukawa Lagrangian term given in equation (4.1) gives rise to a 9×9 mass matrix, which is given in equation 5.1

$$\begin{pmatrix} 0 & 0 & M_D \\ 0 & M_S & M \\ M_D^T & M^T & M_R \end{pmatrix} . \quad (5.1)$$

By considering the mass hierarchy scale as $M_R > M \gg M_D$ we can block diagonalize this 9×9 matrix, and we will finally obtain the mass matrices for the light neutrino, sterile fermion, and right handed neutrino which is given respectively in equations (5.2) .

$$\begin{aligned} m_\nu &= M_D M^{-1} M_S (M_D M^{-1})^T \\ m_S &= M_S - M M_R^{-1} M^T \\ m_R &= M_R . \end{aligned} \quad (5.2)$$

To obtain the eigenvalues we further diagonalized the matrices given in equation (5.2) by their respective unitary matrices as follows

$$\begin{aligned} \hat{m}_\nu &= U_\nu^\dagger m_\nu U_\nu^* = \text{diag}(m_{\nu_1}, m_{\nu_2}, m_{\nu_3}) \\ \hat{m}_S &= U_S^\dagger m_S U_S^* = \text{diag}(m_{S_1}, m_{S_2}, m_{S_3}) \\ \hat{m}_R &= U_N^\dagger m_R U_N^* = \text{diag}(m_{R_1}, m_{R_2}, m_{R_3}) . \end{aligned} \quad (5.3)$$

The complete mixing matrix responsible for diagonalizing the 9 mass matrix given in the equation 5.1 is shown bellow [59, 60, 62]

$$\mathbf{V} = \begin{pmatrix} V^{\nu\nu} & V^{\nu S} & V^{\nu N} \\ V^{S\nu} & V^{SS} & V^{SN} \\ V^{N\nu} & V^{NS} & V^{NN} \end{pmatrix} = \begin{pmatrix} (1 - \frac{1}{2} X X^\dagger) U_\nu & (X - \frac{1}{2} Z Y^\dagger) U_S & Z U_N \\ -X U_\nu & (1 - \frac{1}{2} (X^\dagger X + Y Y^\dagger)) U_S & (Y - \frac{1}{2} X^\dagger Z) U_N \\ y^* X^\dagger U_\nu & -Y^\dagger U_S & (1 - \frac{1}{2} Y^\dagger Y) U_N \end{pmatrix} \quad (5.4)$$

where $X = M_D M^{-1}$, $Y = M M_N^{-1}$, $Z = M_D M_N^{-1}$, and $y = M^{-1} M_S$

Where $U_\nu = V_l^\dagger V_\nu$, but in this model we have considered the charged lepton mass basis is diagonal i.e. V_l

is an identity matrix so $V_\nu = (1 - \eta)U_{PMNS}$ and the parameter η represents the deviation from unitarity. The matrix U_{PMNS} is a unitary matrix and it can be parametrized by using three mixing angles and three phases, among which one is a Dirac CP phase denoted as δ_{CP} and two are Majorana phases (α , β). By using standard parametrization, we can write the U_{PMNS} matrix in the following way

$$U_{PMNS} = \begin{pmatrix} c_{12}c_{13} & s_{12}c_{13} & s_{13}e^{-i\delta_{CP}} \\ -s_{12}c_{23} - c_{12}s_{23}s_{13}e^{i\delta_{CP}} & c_{12}c_{23} - s_{12}s_{23}s_{13}e^{i\delta_{CP}} & s_{23}c_{13} \\ s_{12}s_{23} - c_{12}c_{23}s_{13}e^{i\delta_{CP}} & -c_{12}s_{23} - s_{12}c_{23}s_{13}e^{i\delta_{CP}} & c_{23}c_{13} \end{pmatrix} \begin{pmatrix} 1 & 0 & 0 \\ 0 & e^{i\alpha} & 0 \\ 0 & 0 & e^{i\beta} \end{pmatrix}. \quad (5.5)$$

Where c_{ij} and s_{ij} stands for $\cos \theta_{ij}$ and $\sin \theta_{ij}$, respectively. One can represent all the mixing angles in terms of the elements of the U_{PMNS} matrix as given in equation (5.6), and their 3σ values of neutrino oscillation parameters are given in the Table III. We have used those 3σ ranges for our numerical analysis part.

$$\sin^2 \theta_{13} = |(U_{PMNS})_{13}|^2, \quad \sin^2 \theta_{23} = \frac{|(U_{PMNS})_{23}|^2}{1 - |(U_{PMNS})_{13}|^2}, \quad \sin^2 \theta_{12} = \frac{|(U_{PMNS})_{12}|^2}{1 - |(U_{PMNS})_{13}|^2} \quad (5.6)$$

The Dirac CP phase, Jarlskog invariant and Majorana phases can also be estimated from U_{PMNS} matrix, and their relations are given in the equation (5.7) and (5.8) respectively

$$J_{CP} = \text{Im}[U_{e1}U_{\mu 2}U_{e2}^*U_{\mu 1}^*] = s_{23}c_{23}s_{12}c_{12}s_{13}c_{13}^2 \sin \delta_{CP} \quad (5.7)$$

$$\text{Im}[U_{e1}^*U_{e2}] = c_{12}s_{12}c_{13}^2 \sin \alpha, \quad \text{Im}[U_{e1}^*U_{e3}] = c_{12}s_{13}c_{13} \sin(\beta - \delta_{CP}). \quad (5.8)$$

VI. NON-UNITARY EFFECT

The PMNS matrix is responsible for diagonalizing the light neutrino mass matrix, but in the case of the extended inverse seesaw mechanism, due to the mixing between light and heavy neutrinos even after the diagonalization of the light neutrino mass matrix, we get off-diagonal terms. The complete 9×9 diagonalizing matrix given in the equation (5.4) can be decomposed in the following way [64, 65]

$$\mathbf{V} = \begin{pmatrix} \mathbf{V}_{3 \times 3} & \mathbf{V}_{3 \times 6} \\ \mathbf{V}_{6 \times 3} & \mathbf{V}_{6 \times 6} \end{pmatrix}. \quad (6.1)$$

The PMNS matrix $\mathbf{V}_{3 \times 3} = (1 - \eta)U_\nu$ is responsible for diagonalizing the light neutrino mass matrix, and it is not a unitary matrix. The 3×3 Hermitian matrix $\eta = \frac{1}{2}XX^\dagger$ is known as the deviation from unitarity, which only depends on the Dirac and Majorana matrices of the model. Upper bounds on the elements of this Hermitian matrix [66] have been determined from various experiments, and the 2σ constraints on these values are given below

Oscillation Parameter	Normal Hierarchy	Inverted Hierarchy
$\sin^2 \theta_{12}$	$0.275 \rightarrow 0.345$	$0.275 \rightarrow 0.345$
$\sin^2 \theta_{23}$	$0.435 \rightarrow 0.585$	$0.440 \rightarrow 0.585$
$\sin^2 \theta_{13}$	$0.02030 \rightarrow 0.02388$	$0.02060 \rightarrow 0.02409$
δ_{CP}	$124 \rightarrow 364$	$201 \rightarrow 335$
$\frac{\Delta m_{21}^2}{10^{-5}}$	$6.92 \rightarrow 8.05$	$6.92 \rightarrow 8.05$
$\frac{\Delta m_{3l}^2}{10^{-3}}$	$+2.451 \rightarrow 2.578$	$-2.547 \rightarrow -2.421$

TABLE III: 3σ values of oscillation parameters [63]

$$\eta \leq \begin{pmatrix} 2.5 \times 10^{-3} & 2.4 \times 10^{-5} & 2.7 \times 10^{-3} \\ 2.4 \times 10^{-5} & 4.0 \times 10^{-4} & 1.2 \times 10^{-3} \\ 2.7 \times 10^{-3} & 1.2 \times 10^{-3} & 5.6 \times 10^{-3} \end{pmatrix} \quad (6.2)$$

Due to this non-unitary matrix, the Jarlskog invariant term gets modified, and it can be written in the following way

$$J_{\alpha\beta}^{ij} = \text{Im}(\mathbf{V}_{\alpha i} \mathbf{V}_{\beta j} \mathbf{V}_{\alpha i}^* \mathbf{V}_{\beta j}^*) \approx J_{CP} + \Delta J_{\alpha\beta}^{ij} \quad (6.3)$$

where $\alpha \neq \beta$ and they represent the charged leptons (e, μ, τ), $i \neq j$ and can take the value 1, 2, 3. The first term in the equation (6.3), represents the effect on CP-violation due to the unitary PMNS matrix and the second term represents the contribution to CP-violation due to non-unitary term.

$$\Delta_{\alpha\beta}^{ij} \approx - \sum_{\gamma=e,\mu,\tau} \text{Im}(\eta_{\alpha\gamma} U_{\alpha i} U_{\beta j} U_{\alpha j}^* U_{\beta i}^* + \eta_{\beta\gamma} U_{\alpha i} U_{\gamma j} U_{\alpha j}^* U_{\beta i}^* + \eta_{\alpha\gamma}^* U_{\alpha i} U_{\beta j} U_{\gamma j}^* U_{\beta i}^* + \eta_{\beta\gamma}^* U_{\alpha i} U_{\beta j} U_{\alpha j}^* U_{\gamma i}^*) \quad .$$

Usually, J_{CP} becomes equal to zero when δ_{CP} and $\sin\theta_{13}$ tend to zero but when we consider non-unitary effects Jarlskog invariant term remains non-zero even if δ_{CP} and $\sin\delta_{CP}$ become zero.

VII. NEUTRINOLESS DOUBLE BETA DECAY

Neutrinoless double beta ($0\nu\beta\beta$) is a very fascinating phenomenon in which a nucleus undergoes two successive beta decays without emitting any neutrinos in the final process. This hypothetical nuclear

decay process has not yet been observed. It is a type of beta decay in which two neutrons in the nucleus simultaneously convert into two protons, emitting two electrons but no accompanying neutrinos. The process can be denoted in the following way

$$N(A, Z) \rightarrow N(A, Z + 2) + 2e^-$$

This process violates the conservation of the lepton number, which is an accidental symmetry of the Standard Model. The observation of such decay would imply that neutrinos are their own antiparticles and have a Majorana nature, meaning that the neutrino and antineutrino are indistinguishable. There are several processes that contribute to the $0\nu\beta\beta$ decay in this model. These processes are discussed below

1. *Contribution due to $W_L - W_L$ current*

In the case of $W_L - W_L$ mediation, there are three possible contributions and among them, popular contribution to $0\nu\beta\beta$ decay is the standard contribution i.e. contribution due to the exchange of light Majorana neutrino and the other two contributions are due to the exchange of right-handed and sterile neutrino, which is also known as the non-standard contribution.

2. *Contribution due to $W_R - W_R$ current*

In case when the mediator is purely right-handed current ($W_R - W_R$), there are three potential contributions to neutrinoless double beta decay ($0\nu\beta\beta$). These contributions arise from the exchange of light neutrinos, right-handed, and sterile neutrinos.

3. *Contribution due to $W_L - W_R$ current*

In the case of $W_L - W_R$ mediation, we can have two types of mixed helicity Feynman diagram, which is known as the λ and η diagram.

4. *Contribution due to charged Higgs boson*

The left and right-handed doubly charged Higgs boson namely $\Delta_{L,R}$ also contribute to the $0\nu\beta\beta$ decay but its contribution is negligible as compared to other processes.

The Feynman diagram and amplitude of all the above mention processes are given in the Appendix A.

VIII. NUMERICAL ANALYSIS AND RESULTS

In case of Extended inverse seesaw mechanism the light neutrino mass matrix is given by

$$m_\nu = M_D M^{-1} M_S (M_D M^{-1})^T \quad (8.1)$$

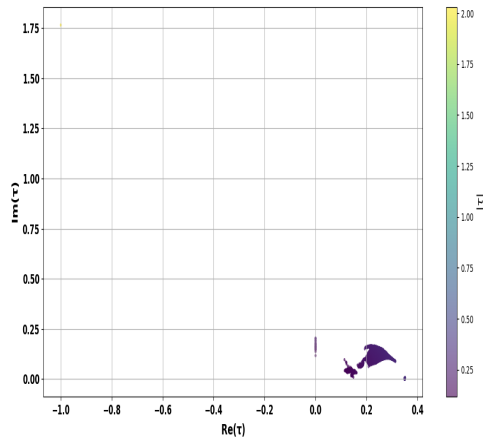
We can also write light neutrino mass matrix in terms of U_{PMNS} matrix in the following way

$$m_\nu = (1 - \eta) U_{PMNS} m_{dig} ((1 - \eta) U_{PMNS})^\dagger \quad (8.2)$$

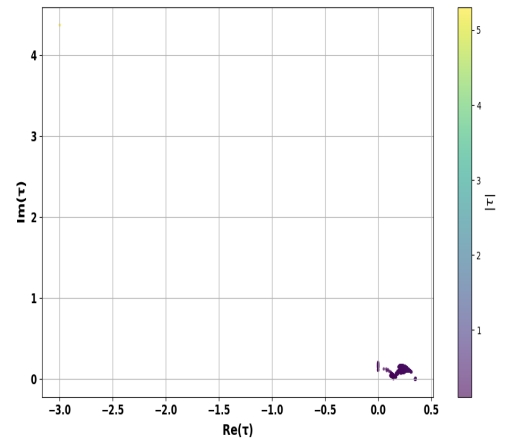
After constructing the mass matrices utilizing the multiplication rules of the A_4 group, we incorporated these matrices into equation (8.1) to derive the light neutrino mass matrix in terms of Yukawa couplings. To further analyze this, we computed the values of the Yukawa couplings using the 3σ values of oscillation parameters, which were then inserted into equation (8.2). Subsequently, we equated equations (8.1) and (8.2) to determine the unknown values of the Yukawa couplings. Table IV provides the Yukawa coupling values.

Yukawa coupling	for NH	for IH
$Y_{3,1}^{(0)}$	$0.00069 - 6.725$	$0.00171 - 8.829$
$Y_{3,2}^{(0)}$	$0.00098 - 6.362$	$0.00090 - 6.783$
$Y_{3,3}^{(0)}$	$0.00025 - 6.226$	$0.00041 - 6.700$

TABLE IV: Yukawa coupling values for NH and IH



(a) Variation of $\text{Re}\tau$ and $\text{Im}\tau$



(b) Variation of $\text{Re}\tau$ and $\text{Im}\tau$

FIG. 1: The two figures show the parameter space for the real and imaginary parts of the modulus τ for NH and IH, respectively.

The motivation behind utilizing the modular group is to minimize the necessity of introducing an additional field, commonly known as a "flavon", for breaking the discrete flavor symmetry. Within modular symmetry, the modulus τ is responsible for breaking the discrete flavor symmetry. We calculated the values of the modulus τ by employing the q expansion of the modular form as given in equation (3.7). We have computed the absolute value of the modulus τ , as well as its real and imaginary components, from our model. For the NH case, the real part of τ ranges from -0.999 to 0.35 , and the imaginary part ranges from 2.8×10^{-5} to 1.764 . However, as shown in Figure 1a, we observe that most of the real part values of τ are concentrated within the range 0.1 to 0.3 , while the imaginary part predominantly spans from 2.8×10^{-5} to below 0.25 . Similarly, for the IH case, the computed real part of τ lies within the range -3.0 to 0.35 , and the imaginary part spans 1.5×10^{-5} to 4.37 . However, Figure 1b indicates that the real part of τ is primarily clustered between 0.1 and 0.4 , while the imaginary part mostly occupies the range 1.5×10^{-5} to 0.2 . Additionally, Figure 1 provides insight into the parameter space of the absolute value of τ . We find that, in the case of NH, the modulus $|\tau|$ ranges from 0.117 to 2.028 , whereas for IH, it spans from 0.109 to 5.302 .

A. Active neutrino masses

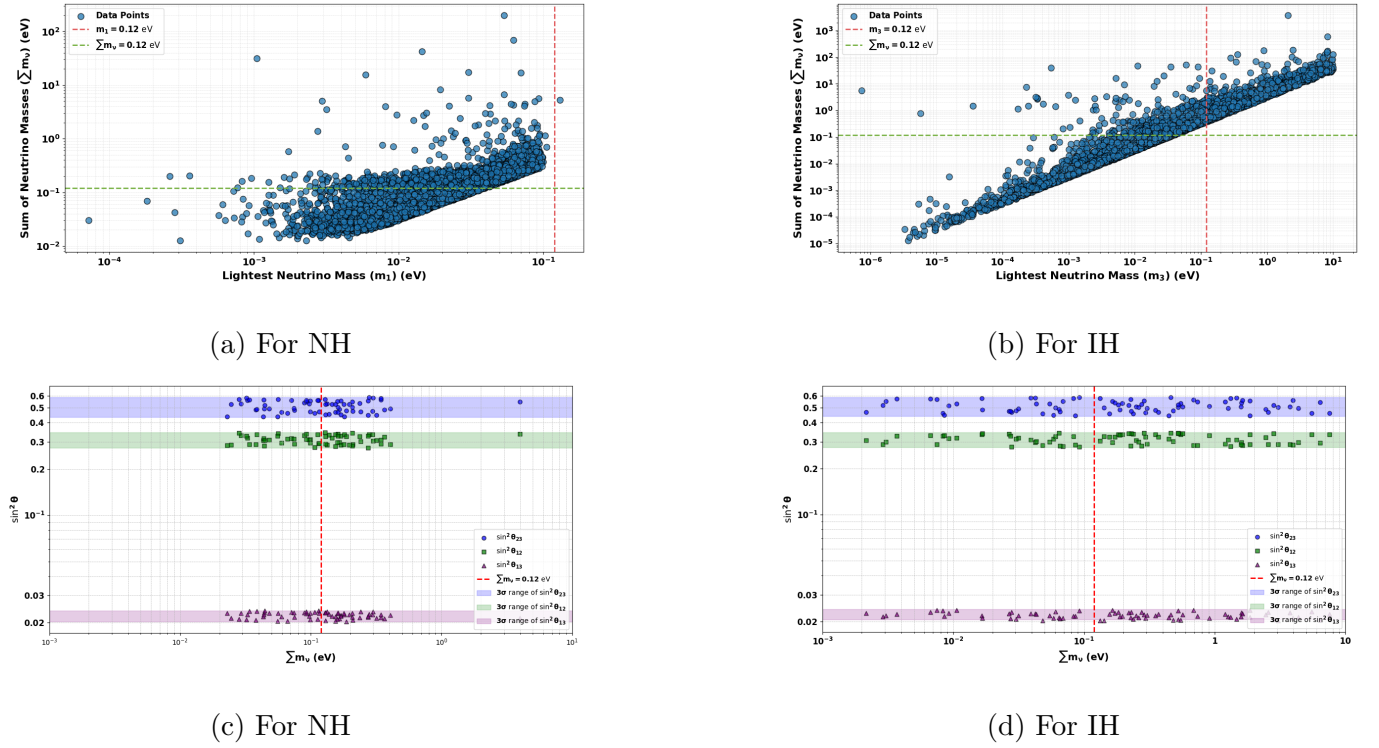
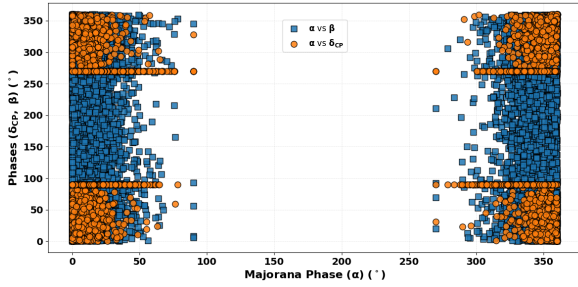
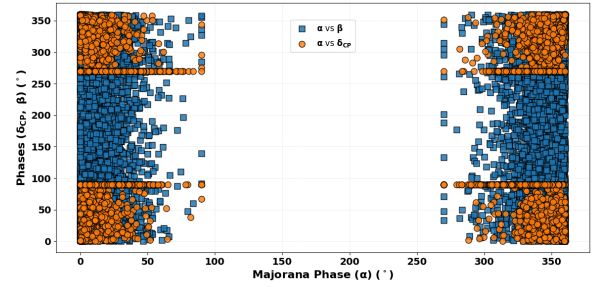


FIG. 2: The top two Figures show variations of sum of the neutrino masses with the lightest neutrino mass for NH and IH and the bottom two Figures show the variation of mixing angles with the sum of the neutrino masses for NH and IH.



(a) For NH



(b) For IH

FIG. 3: Figures show the parameter space of δ_{CP} and Majorana phases (α and β) for NH and IH.

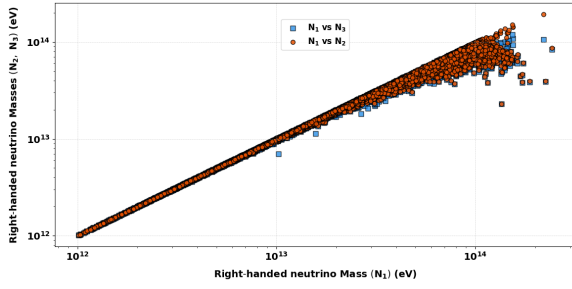
We have plotted a graph depicting the relationship between the sum of neutrino masses and the lightest neutrino mass, considering both the normal and inverted hierarchies. It appears that the majority of the calculated values lie below the experimental bound. This experimental bound is represented by a horizontal and vertical lines in Figures 2a and 2b. To verify the consistency of the model, we have also plotted the mixing angles calculated from the model against the sum of the neutrino masses for both NH and IH. Figures 2c and 2d show the variation of the three mixing angles with the sum of the neutrino masses for NH and IH respectively. We have observed that most of the data fall within the experimental 3σ range. We have also calculated the value of the two Majorana phases and δ_{CP} from our model. From Figures 3a and 3b, it is observed that the Majorana phase α lies within the range of $[0^\circ - 50^\circ]$ and $[300^\circ - 350^\circ]$, moreover δ_{CP} values are same as those of the Majorana phase α . Majorana phase β covers all values from 0° to 350° and it holds true for both the NH and IH cases.

B. Heavy neutrino Eigenstates

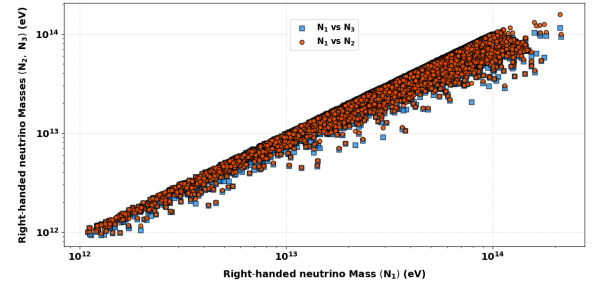
Within this model, we have a total of six heavy mass eigenstates, comprising three right-handed neutrinos and three sterile fermions. To analyze the parameter space for right-handed neutrino masses, we have plotted the variation of M_{N_1} against M_{N_2} and M_{N_3} for both NH and IH. The model predicts that the right-handed neutrino masses range from 1 TeV to 100 TeV. Similarly, we have studied the parameter space for the masses of sterile fermions. As shown in Figures 5a and 5b, the sterile fermion masses range from 0.01 TeV to approximately 10^4 TeV and, it holds true for both NH and IH.

C. Effective neutrino mass and Half life of $0\nu\beta\beta$ decay

In Section VII, we have briefly discussed all the contributions to $0\nu\beta\beta$ decay associated with our model and in this section, we have discussed effective mass and its corresponding half-life and done a detailed numerical analysis of all the contributions. We have plotted graphs showing the variation of the

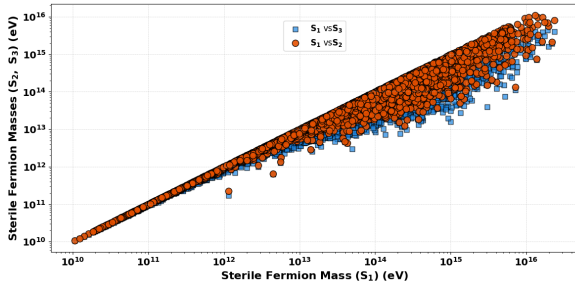


(a) For NH

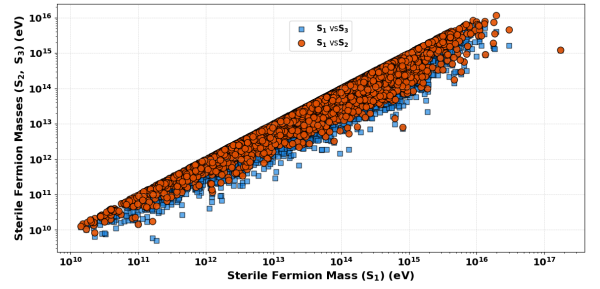


(b) For IH

FIG. 4: The two Figures show the parameter space for RH neutrino masses.



(a) For NH



(b) For IH

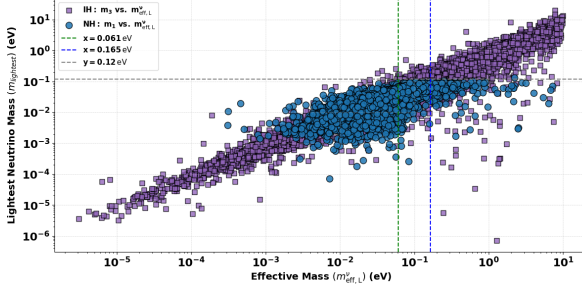
FIG. 5: The two Figures show the parameter space for sterile fermion masses.

effective mass of $0\nu\beta\beta$ decay and its corresponding half-life of $(0\nu\beta\beta)$ decay with the lightest neutrino mass, considering both standard and non-standard contributions. In all the plots, which represent the variation of effective mass with the lightest neutrino mass, the presence of a horizontal line indicates the Planck constraint on the total sum of neutrino masses, while the two vertical lines represent the uncertainty on the effective mass due to nuclear mass matrix and effective mass should be less than this bound. Similarly, in all the figures, related to the half-life of $0\nu\beta\beta$ the horizontal line represents the Planck constraint, whereas the two vertical lines indicate the experimental bounds on the half-life for the isotope Xe^{136} . Different experimental bounds on the half-life of $0\nu\beta\beta$ for the isotopes Ge and Xe are given in Table V. As already mentioned within the left-right asymmetric framework, gauge coupling, g_l and g_r are not equal and their values depend upon the symmetry-breaking chain. Due to an unequal gauge coupling, we can see that an extra term $(\frac{g_r}{g_l})$ appears in the calculation of effective Majorana mass and half-life of $0\nu\beta\beta$ decay. We have considered the ratio $\frac{g_r}{g_l}$ equal to 0.6 [67] and the right-handed gauge boson mass M_{W_R} of 3 TeV. A detailed discussion about the effective Majorana mass and half-life of $0\nu\beta\beta$ is given in the Appendix A and B respectively.

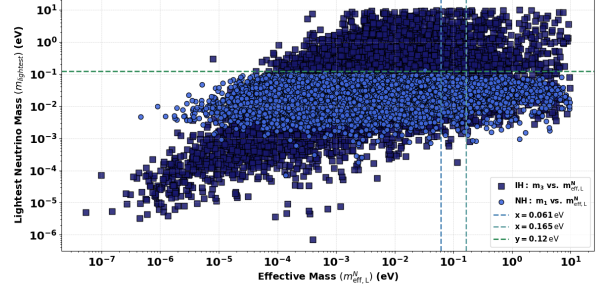
Isotope	^{76}Ge	^{136}Xe	^{136}Xe	^{136}Xe
$T_{1/2}^{0\nu}[\text{years}]$	$> 1.8 \times 10^{26}$	3.5×10^{25}	$> 1.9 \times 10^{25}$	$> 2.3 \times 10^{26}$
Experiment	GERDA [68]	EXO [69]	KamLAND-Zen [70]	EXO + KamLAND-Zen [71]

TABLE V: Experimental bounds on half-life

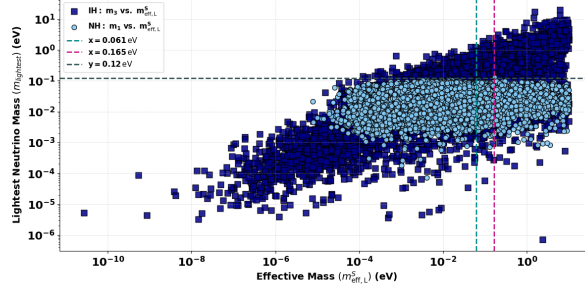
1. *Effective mass and half-life due to $W_L - W_L$ current*



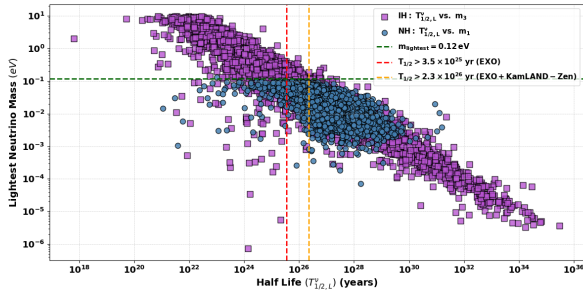
(a) m_{eff} due to light neutrino exchange



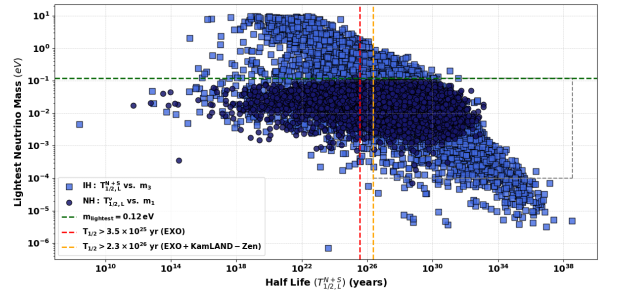
(b) m_{eff} due to RH neutrino exchange



(c) m_{eff} due to sterile fermion exchange



(d) Half life due to standard contribution



(e) Half life due to non standard contribution

FIG. 6: The top three Figures show the variation of effective mass with the lightest neutrino mass for NH and IH. The bottom two Figures show the variation of Half-life of $0\nu\beta\beta$ decay with lightest neutrino mass for NH and IH

The effective Majorana mass and half life due to exchange of light neutrino and heavy neutrino in case of $W_L - W_L$ current are given in the equation (8.3) and (8.4) respectively

$$m_{ee,L}^\nu = \sum_{i=1}^3 V_{ei}^{\nu\nu^2} m_{\nu i}, \quad m_{ee,L}^N = \sum_{i=1}^3 V_{ei}^{\nu N^2} \frac{|p|^2}{M_{N_i}}, \quad m_{ee,L}^S = \sum_{i=1}^3 V_{ei}^{\nu S^2} \frac{|p|^2}{M_{S_i}}. \quad (8.3)$$

$$[T_{1/2}^{0\nu}]^{-1} = \mathcal{K}_{0\nu} \left[|m_{ee,L}^\nu|^2 + |m_{ee,L}^S + m_{ee,L}^N|^2 \right] \quad (8.4)$$

We have calculated the effective Majorana mass and its corresponding half-life of $0\nu\beta\beta$ for $W_L - W_L$ mediation due to the exchange of light neutrino, RH neutrino, and sterile neutrino and plotted those calculated values against lightest neutrino mass. In Figures 6a, 6b, and 6c, we have observed that most of the calculated values of the effective mass due to light, heavy RH, and sterile neutrino exchange fall well below the experimental bound. In the case of NH, the model predicts the lower bound on the effective Majorana mass to be of the order of 10^{-3} to 10^{-4} when the exchange particle is a light or sterile neutrino, and approximately of the order of 10^{-6} when the exchange particle is a RH neutrino. However, in the case of IH, the lower bound predicted by the model due to the exchange of light neutrino, heavy RH neutrino, and sterile neutrino is approximately of the order of 10^{-5} to 10^{-8} , which is smaller compared to the NH case. We have also calculated the half-life of $0\nu\beta\beta$ decay due to light neutrino exchange and due to the exchange of heavy neutrinos for NH and IH, which is shown in Figure 6d and 6e respectively.

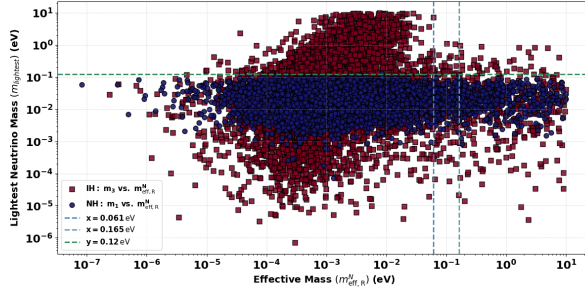
2. Effective mass and half-life due to $W_R - W_R$ current

The effective Majorana mass and half life due to exchange of light neutrino and heavy neutrino in case of purely right handed current are given in the equation (8.5) and (8.6) respectively

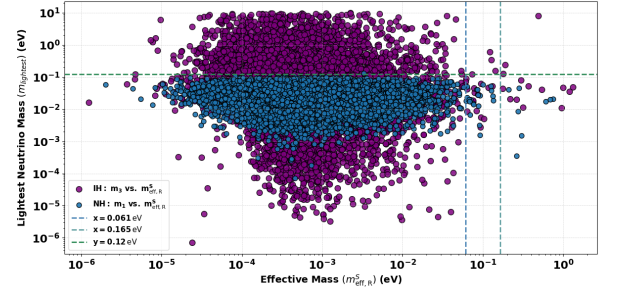
$$\begin{aligned} m_{ee,R}^\nu &= \left(\frac{M_{W_L}}{M_{W_R}} \right)^4 \left(\frac{g_r}{g_l} \right)^4 \sum_{i=1}^3 V_{ei}^{N\nu^2} m_{\nu i} \\ m_{ee,R}^N &= \left(\frac{M_{W_L}}{M_{W_R}} \right)^4 \left(\frac{g_r}{g_l} \right)^4 \sum_{i=1}^3 V_{ei}^{NN^2} \frac{|p|^2}{M_{N_i}} \\ m_{ee,R}^S &= \left(\frac{M_{W_L}}{M_{W_R}} \right)^4 \left(\frac{g_r}{g_l} \right)^4 \sum_{i=1}^3 V_{ei}^{NS^2} \frac{|p|^2}{M_{S_i}} \end{aligned} \quad (8.5)$$

$$[T_{1/2}^{0\nu}]^{-1} = \mathcal{K}_{0\nu} \left[|m_{ee,R}^\nu + m_{ee,R}^S + m_{ee,R}^N|^2 \right] \quad (8.6)$$

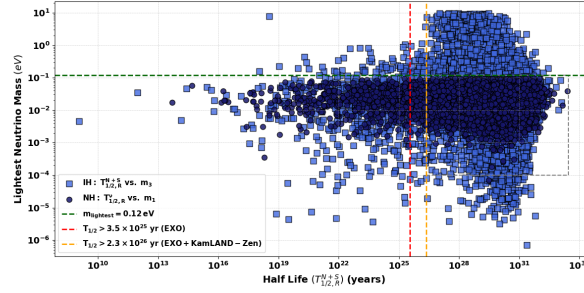
We have calculated the effective Majorana mass and corresponding half-life for the $(0\nu\beta\beta)$ decay mediated by $W_R - W_R$ interactions, considering the exchange of light neutrinos, RH, and sterile neutrinos. In Figures 7a and 7b, we observed that the calculated effective masses due to RH and sterile neutrino exchanges consistently fall below the experimental bounds. Notably, the contribution from the exchange of light neutrinos via $W_R - W_R$ currents was found to be significantly smaller compared to



(a) m_{eff} due to the exchange of RH neutrino



(b) m_{eff} due to the exchange of sterile fermion



(c) Half life due to non standard contribution

FIG. 7: The top two figures show the variation of effective mass with the lightest neutrino mass for NH and IH. The bottom Figure show the variation of half-life with the lightest neutrino mass for NH and IH

other mechanisms, resulting in a very large corresponding half-life. Given this negligible contribution, we have omitted it from our total half-life calculations related to $W_R - W_R$ interactions. In Figure 7c, we have depicted the calculated half-lives for $(0\nu\beta\beta)$ decay resulting from heavy neutrino exchanges, plotted against the lightest neutrino mass for both NH and IH scenarios.

D. Calculation of non-unitary matrix and J_{CP}

Due to the presence of heavy RH and sterile neutrinos we obtain a non-unitary PMNS matrix and the term $\eta = \frac{1}{2}XX^\dagger$ represents the deviation from unitarity. Our calculations show that the deviations from unitarity, represented by the elements of the η matrix, predominantly lie within the range of 10^{-3} to 10^{-9} , which remain well below the current experimental bounds for the NH. For the IH, the calculated values span a broader range, from 10^{-2} to 10^{-11} . Table VI presents the computed lower and upper bounds for each element of the matrix. Examining the CP violation terms resulting from non-unitarity, we find that for NH, $J_{e\mu}^{13}$ is equal to $J_{e\mu}^{32}$ and their values range from -2.1×10^{-4} to 8.7×10^{-6} . We have also get equal value for $J_{e\mu}^{31}$ and $J_{e\mu}^{23}$ and their values vary from -8.7×10^{-6} to 2.1×10^{-4} . For IH, we find that $J_{e\mu}^{13}$ values range from -2.3×10^{-3} to 6.4×10^{-4} and $J_{e\mu}^{31}$ values range from -6.4×10^{-4} to

η_{ij}	NH Min	NH Max	IH Min	IH Max
η_{ee}	9.94×10^{-8}	2.3×10^{-3}	8.92×10^{-11}	2.4×10^{-2}
$\eta_{e\mu}$	3.9×10^{-9}	1.2×10^{-3}	3.2×10^{-11}	2.4×10^{-2}
$\eta_{e\tau}$	1.7×10^{-9}	1.2×10^{-3}	3.5×10^{-11}	2.1×10^{-2}
$\eta_{\mu\mu}$	8.8×10^{-8}	2.3×10^{-3}	1.5×10^{-10}	5.5×10^{-2}
$\eta_{\mu\tau}$	1.02×10^{-9}	2.2×10^{-3}	3.8×10^{-11}	2.9×10^{-2}
$\eta_{\tau\tau}$	8.8×10^{-8}	3.8×10^{-3}	1.7×10^{-10}	8.1×10^{-2}

TABLE VI: Minimum and maximum values of the elements of the non-unitary matrix η_{ij} for NH and IH.

$\Delta J_{\alpha\beta}^{ij}$	NH (Min)	NH (Max)	IH (Min)	IH (Max)
$\Delta J_{e\mu}^{21}$	-5.1×10^{-4}	8.9×10^{-6}	-3.3×10^{-3}	1.5×10^{-3}
$\Delta J_{e\mu}^{13}$	-2.2×10^{-4}	8.7×10^{-6}	-2.3×10^{-3}	6.4×10^{-4}
$\Delta J_{e\tau}^{12}$	-1.2×10^{-5}	1.1×10^{-4}	-5.7×10^{-4}	1.6×10^{-3}
$\Delta J_{\mu e}^{13}$	-5.9×10^{-6}	2.5×10^{-4}	-7.6×10^{-4}	2.3×10^{-3}
$\Delta J_{\mu\tau}^{12}$	-1.2×10^{-4}	7.3×10^{-5}	-1.7×10^{-3}	1.8×10^{-3}
$\Delta J_{\tau e}^{31}$	-2.2×10^{-4}	2.4×10^{-5}	-1.6×10^{-3}	1.6×10^{-4}

TABLE VII: Calculated minimum and maximum values of $\Delta J_{\alpha\beta}^{ij}$ for both NH and IH.

2.3×10^{-3} . Additionally, we observe that the absolute values of $J_{e\tau}^{ij}$ are equal. A Similar result is also observed for $J_{\mu\tau}^{ij}$, where $i \neq j$ and it can take values from 1 to 3. The Calculated CP violation term due to non-unitary effects are given in Table VII.

IX. CONCLUSION

We have developed a non-supersymmetric model using the concept of modular symmetry, where the usual requirement of holomorphicity is replaced by the Laplacian condition. The Yukawa couplings in this model include both holomorphic and non-holomorphic parts. We have studied the left-right asymmetric model, where we have used the intermediate gauge group $SU(2)_R \times U(1)_R \times U(1)_{B-L}$ to explore the neutrino masses and mixing by using the Γ_3 modular group, which is isomorphic to the A_4 discrete symmetric group. From the calculated Yukawa couplings obtained from the model for both NH and IH, we determined the real, imaginary, and absolute values of the modulus τ using the q -expansion of modular forms. We found that, in the case of NH, most of the values of real part of τ lies in the range 0.1 to 0.3, while the imaginary part falls within the upper half of the complex plane, ranging from 2.8×10^{-5} to 0.25. For IH, the real part of τ lies between 0.1 and 0.4, and the imaginary part ranges from -1.5×10^{-5} to 0.2. Additionally, the absolute value of τ is found to range from 0.117 to 2.028 in the case of NH, and from 0.109 to 5.302 in the case of IH. We have generated the light neutrino mass by using an extended inverse seesaw mechanism and for that purpose, we have introduced one sterile fermion per generation. The model predicts the sum of neutrino masses, with values well below experimental bounds for both NH and IH. The model predicts the lower bound on the lightest neutrino mass for NH to be approximately 10^{-4} eV, and around 10^{-5} eV for IH. In addition to neutrino masses, the model successfully predicts the mixing angles within the 3σ range. Furthermore, it predicts that the δ_{CP} phase is similar to one of the Majorana phases, denoted as α in the model. Additionally, we calculated effective mass and half-lives due to the mediation of $W_L - W_L$, and $W_R - W_R$ contribution. We have observed that the analytical formula for effective mass gets modified for $W_R - W_R$ mediation and depend on the ratio $\frac{g_r}{g_l}$. All the calculated values of the effective mass parameter and its corresponding half-lives due to standard and non-standard contributions are found to lie in the experimental allowed region for both the NH and IH cases. From our analysis, we find that in the case of the $W_L - W_L$ current, the model predicts the effective Majorana mass to lie within the range of 10^{-3} eV to 10^{-4} eV, and the half-life of the $0\nu\beta\beta$ decay to fall within the range of 10^{28} to 10^{30} years for the NH. In contrast, for the IH, the effective Majorana mass is predicted to lie within the range of 10^{-5} eV to 10^{-6} eV, with the corresponding half-life ranging from 10^{32} to 10^{34} years. Similarly, in the case of the $W_R - W_R$ current, the model predicts that the effective Majorana mass, arising from the exchange of heavy RH neutrinos and sterile neutrinos, lies within the range of 10^{-4} eV to 10^{-5} eV for both NH and IH. The corresponding half-life of the $0\nu\beta\beta$ decay is found to lie in the range of 10^{31} to 10^{32} years, which holds true for both hierarchies. Furthermore, we analyzed deviations from unitarity in the relevant matrix elements, finding them within the range of 10^{-3} to 10^{-9} .

In conclusion, our non-supersymmetric left-right asymmetric model, based on the framework of auto-

morphic forms, successfully predicts neutrino oscillation parameters and the effective mass and half-life of neutrinoless double beta decay.

Appendix A: Feynman diagram and Feynman amplitude for different contribution to $0\nu\beta\beta$ decay

a. Contribution due to $W_L - W_L$ current

The Feynman diagram associated with those contributions are given in Figure 8 and the associated Feynman amplitude and its corresponding lepton number violating (LNV) particle physics parameter are given in the equation (A1), and (A2) respectively.

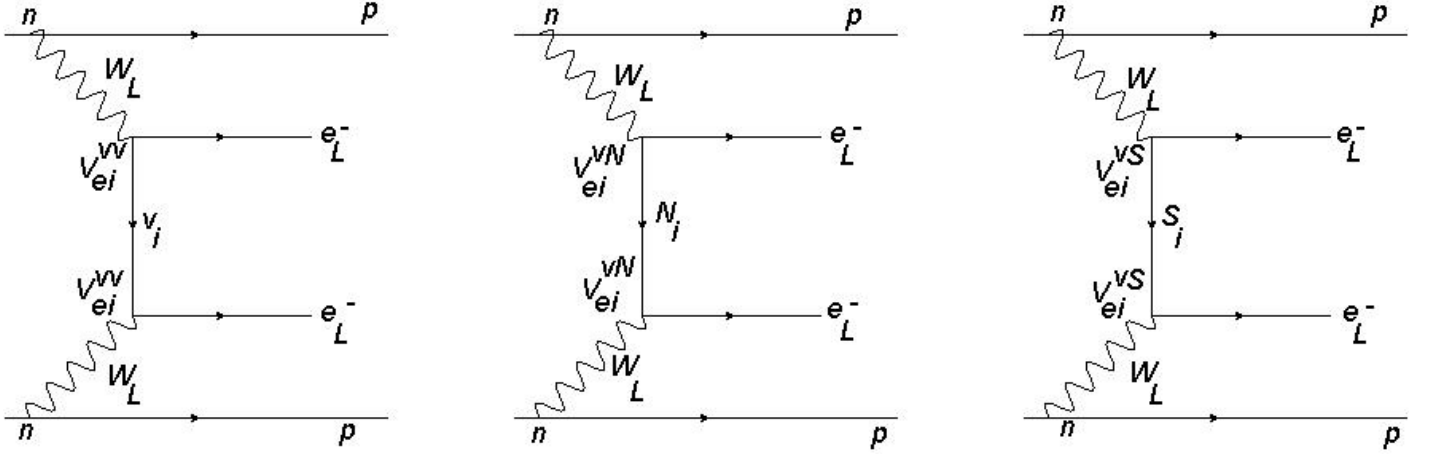


FIG. 8: Feynman diagram for $W_L - W_L$ mediation

$$\mathcal{A}_{LL}^\nu \propto G_R^2 \sum_{i=1,2,3} \frac{V_{ei}^{\nu\nu} m_{\nu_i}}{p^2}, \quad \mathcal{A}_{LL}^N \propto G_F^2 \sum_{i=1,2,3} \left(-\frac{V_{ei}^{\nu N^2}}{M_{N_i}} \right), \quad \mathcal{A}_{LL}^S \propto G_F^2 \sum_{i=1,2,3} \left(-\frac{V_{ek}^{\nu S^2}}{M_{S_k}} \right) \quad (\text{A1})$$

where $G_F = 1.2 \times 10^{-5} \text{GeV}^{-2}$ is the Fermi coupling constant.

$$|\eta_{LL}^\nu| = \sum_{i=1,2,3} \frac{V_{ei}^{\nu\nu^2} m_{\nu_i}}{m_e}, \quad |\eta_{LL}^N| = m_p \sum_{i=1,2,3} \frac{V_{ei}^{\nu N^2}}{M_{N_i}}, \quad |\eta_{LL}^S| = m_p \sum_{i=1,2,3} \frac{V_{ei}^{\nu S^2}}{M_{S_i}} \quad (\text{A2})$$

b. Contribution due to $W_R - W_R$ current

The Feynman diagram for those contributions are given in Figure 9. Equations(A3) and (A4) provide the amplitude of those diagrams and LNV parameters respectively.

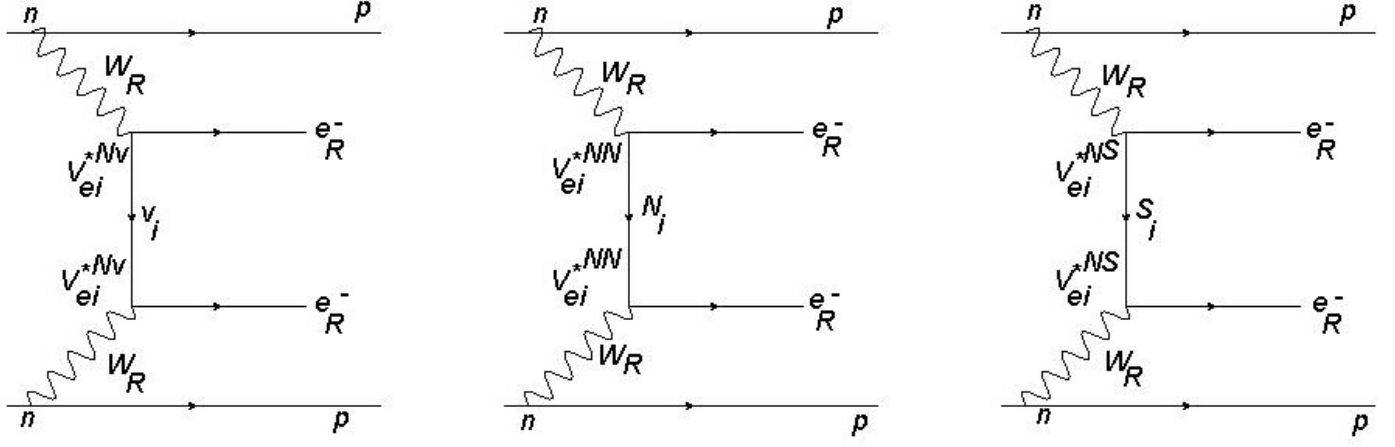


FIG. 9: Feynman diagram for $W_R - W_R$

$$\begin{aligned}
\mathcal{A}_{RR}^{\nu} &\propto G_F^2 \sum_{i=1,2,3} \left(\frac{M_{W_L}}{M_{W_R}} \right)^4 \left(\frac{g_r}{g_l} \right)^4 \frac{V_{ei}^{N\nu^2} m_{\nu_i}}{p^2} \\
\mathcal{A}_{RR}^N &\propto G_F^2 \sum_{j=1,2,3} \left(\frac{M_{W_L}}{M_{W_R}} \right)^4 \left(\frac{g_r}{g_l} \right)^4 \left(-\frac{V_{ej}^{NN^2}}{M_{N_j}} \right) \\
\mathcal{A}_{RR}^S &\propto G_F^2 \sum_{k=1,2,3} \left(\frac{M_{W_L}}{M_{W_R}} \right)^4 \left(\frac{g_r}{g_l} \right)^4 \left(-\frac{V_{ek}^{NS^2}}{M_{S_k}} \right)
\end{aligned} \tag{A3}$$

$$\begin{aligned}
|\eta|_{RR}^{\nu} &= \sum_{i=1,2,3} \left(\frac{M_{W_L}}{M_{W_R}} \right)^4 \left(\frac{g_r}{g_l} \right)^4 \frac{V_{ei}^{N\nu^2} m_{\nu_i}}{m_e} \\
|\eta|_{RR}^N &= \sum_{i=1,2,3} m_p \left(\frac{M_{W_L}}{M_{W_R}} \right)^4 \left(\frac{g_r}{g_l} \right)^4 \left(\frac{V_{ei}^{NN^2}}{M_{N_i}} \right) \\
|\eta|_{RR}^S &= \sum_{i=1,2,3} m_p \left(\frac{M_{W_L}}{M_{W_R}} \right)^4 \left(\frac{g_r}{g_l} \right)^4 \left(\frac{V_{ei}^{NS^2}}{M_{S_i}} \right)
\end{aligned} \tag{A4}$$

c. Contribution due to $W_L - W_R$ current

In case of $W_L - W_R$ mediation, we can have two type of mixed helicity Feynman diagram, which is known as the λ and η diagram. The Feynman diagram associated with those contribution is given in the Figure 10 and 11 respectively.

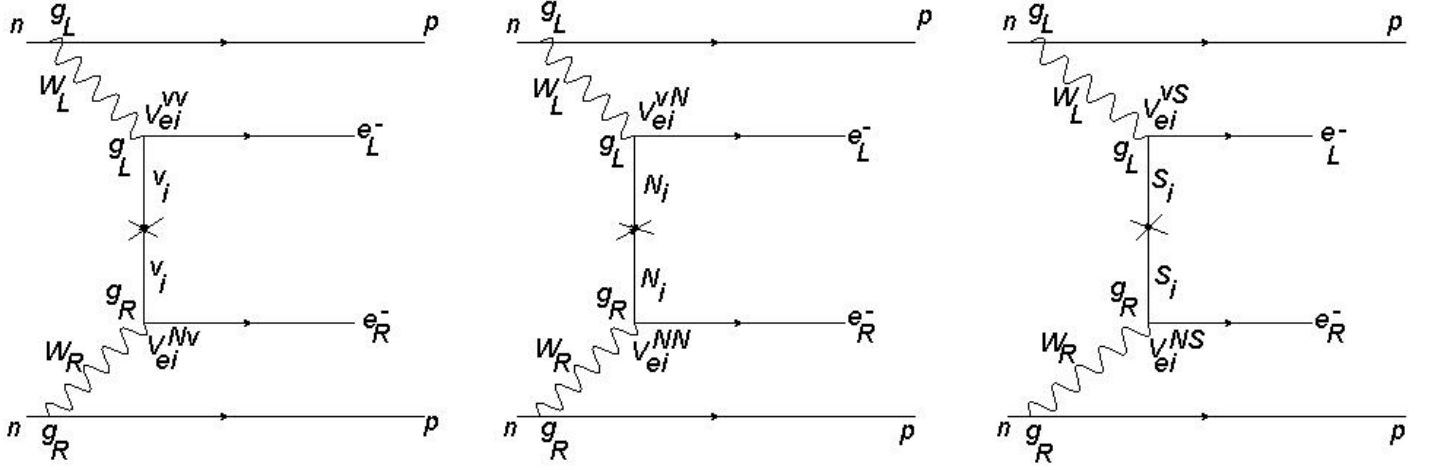


FIG. 10: Feynman diagram for λ

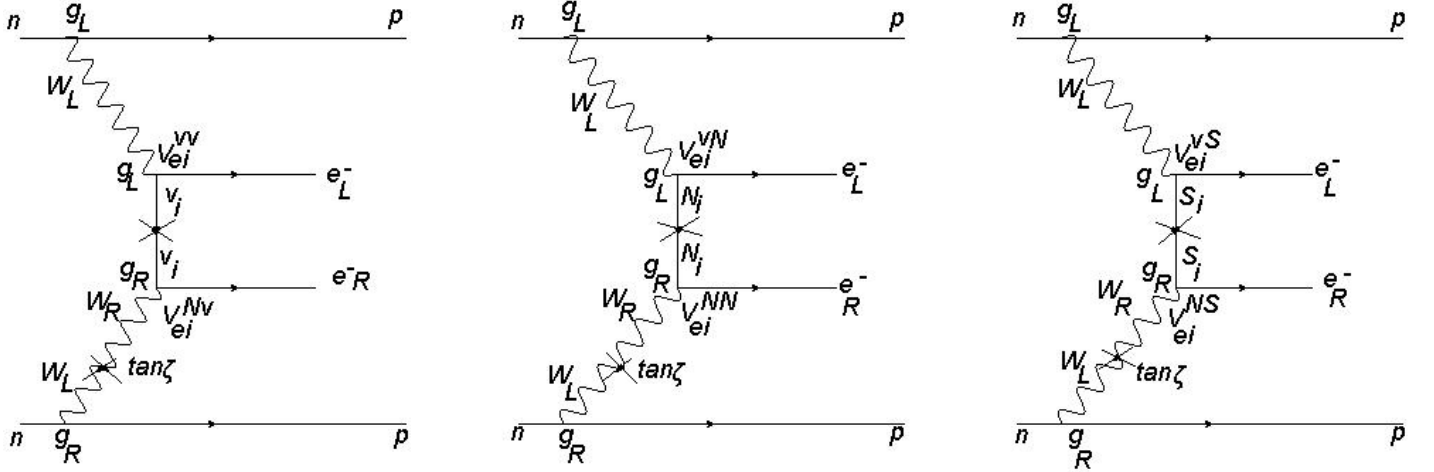


FIG. 11: Feynman diagram for η

1 Feynman amplitudes for λ - mechanism

$$\begin{aligned}
 \mathcal{A}_\lambda^\nu &\propto G_F^2 \left(\frac{M_{W_L}}{M_{W_R}} \right)^2 \left(\frac{g_r}{g_l} \right)^2 \sum_{i=1,2,3} V_{ei}^{\nu\nu} V_{ei}^{N\nu} \frac{1}{|p|} \\
 \mathcal{A}_\lambda^N &\propto G_F^2 \left(\frac{M_{W_L}}{M_{W_R}} \right)^2 \left(\frac{g_r}{g_l} \right)^2 \sum_{j=1,2,3} V_{ej}^{\nu N} V_{ej}^{NN} \frac{|p|}{M_{N_j}^2} \\
 \mathcal{A}_\lambda^N &\propto G_F^2 \left(\frac{M_{W_L}}{M_{W_R}} \right)^2 \left(\frac{g_r}{g_l} \right)^2 \sum_{k=1,2,3} V_{ek}^{\nu\nu} V_{ek}^{NS} \frac{|p|}{M_{S_k}^2}
 \end{aligned} \tag{A5}$$

2 Feynman amplitudes for η -mechanism

$$\begin{aligned}
\mathcal{A}_\lambda^\nu &\propto G_F^2 \left(\frac{g_r}{g_l}\right) \text{ten} \zeta \sum_{i=1,2,3} V_{ei}^{\nu\nu} V_{ei}^{N\nu} \frac{1}{|p|} \\
\mathcal{A}_\lambda^N &\propto G_F^2 \left(\frac{g_r}{g_l}\right) \text{ten} \zeta \sum_{j=1,2,3} V_{ej}^{\nu N} V_{ej}^{NN} \frac{|p|}{M_{N_j}^2} \\
\mathcal{A}_\lambda^S &\propto G_F^2 \left(\frac{g_r}{g_l}\right) \text{ten} \zeta \sum_{k=1,2,3} V_{ek}^{\nu S} V_{ek}^{NS} \frac{|p|}{M_{S_k}^2}
\end{aligned} \tag{A6}$$

d. Contribution due to doubly charged Higgs boson

The Feynman amplitude and diagram due to doubly charged Higgs boson are given in equation A7 and in Figure 12 respectively

$$\begin{aligned}
\mathcal{A}_{LL}^{\Delta_L} &\propto G_F^2 \sum_{i=1,2,3} \frac{1}{M_{\Delta_L}^2} V_{ei}^{\nu\nu^2} m_{\nu_i} \\
\mathcal{A}_{RR}^{\Delta_R} &\propto G_F^2 \sum_{i=1,2,3} \left(\frac{M_{W_L}}{M_{W_R}}\right)^4 \left(\frac{g_r}{g_l}\right)^4 \frac{1}{M_{\Delta_R}^2} V_{ei}^{NN^2} M_{N_i}
\end{aligned} \tag{A7}$$

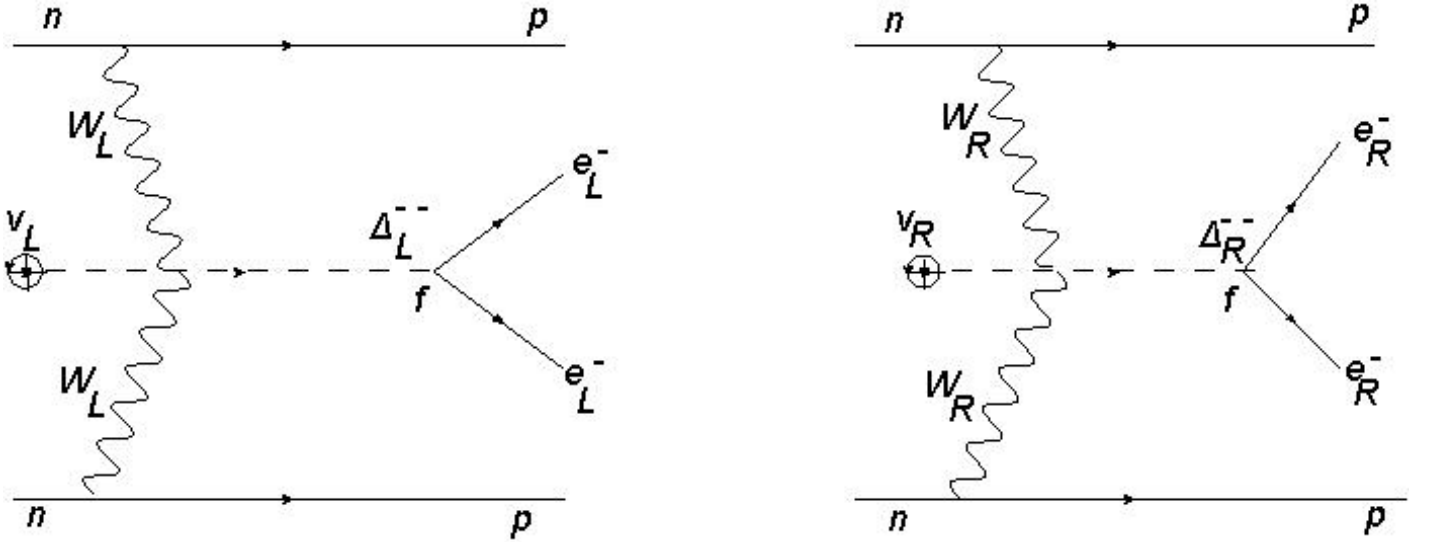


FIG. 12: Feynman diagram for doubly charged Higgs boson

Appendix B: Half-life of $0\nu\beta\beta$ decay

The analytic expression for the inverse half life of neutrino less double beta decay considering all the contribution can be written in the following way [72, 73]

$$[T_{1/2}^\nu]^{-1} = G_{01}^{0\nu} |M_\nu^{0\nu}|^2 |\eta_{LL}^\nu|^2 + |M_N^{0\nu}|^2 |\eta_{LL}^{N,S}|^2 + |M_\nu^{0\nu}|^2 |\eta_{RR}^\nu|^2 + |M_N^{0\nu}|^2 |\eta_{RR}^{N,S}|^2 + |M_\lambda^{0\nu} \eta_\lambda + M_\eta^{0\nu} \eta_\eta|^2. \tag{B1}$$

Where $G_{01}^{0\nu}$ is the phase space factor and $M_i^{0\nu}(i = \nu, N, \lambda, \eta)$ is the nuclear matrix elements and $|\eta|$ is a dimensionless parameter. The experimental values of nuclear mass matrix for the isotope Ge and Xe is given in the Table VIII. Considering only the standard contribution due to the exchange of light Majorana neutrino we can write inverse half life formula in the following way [67]

$$[T_{1/2}^\nu]^{-1} = G_{01}^{0\nu} |M_\nu^{0\nu}|^2 |\eta_{LL}^\nu|^2 \quad (\text{B2})$$

and by using equation (A2), one can modify equation (B2) in terms of effective mass $|m_{ee,L}^\nu|$

$$[T_{1/2}^\nu]^{-1} = G_{01}^{0\nu} \left| \frac{M_\nu^{0\nu}}{m_e} \right|^2 |m_{ee,L}^\nu|^2 \quad (\text{B3})$$

where, m_e is mass of the electron. One can take the term $\mathcal{K}_{0\nu} = G_{01}^{0\nu} \left| \frac{M_\nu^{0\nu}}{m_e} \right|^2$ as a normalizing factor for other contribution and can write equation (B1) in terms of the effective Majorana mass parameter in the following way

Isotope	$G_{01}^{0\nu}$	$M_\nu^{0\nu}$	$M_N^{0\nu}$	$M_\lambda^{0\nu}$	$M_\eta^{0\nu}$
76_{Ge}	5.77×10^{-15}	$2.58 - 6.64$	$233 - 412$	$1.75 - 3.76$	$235 - 637$
136_{Xe}	3.56×10^{-14}	$1.57 - 3.85$	$164 - 172$	$1.92 - 2.49$	$370 - 419$

TABLE VIII: Allowed ranges of phase space factors and nuclear matrix elements[59]

$$[T_{1/2}^{0\nu}]^{-1} = \mathcal{K}_{0\nu} \left[|m_{ee,L}^\nu|^2 + |m_{ee,L}^S + m_{ee,L}^N|^2 + |m_{ee,R}^\nu + m_{ee,R}^S + m_{ee,R}^N|^2 + |m_{ee,\lambda}^\nu + m_{ee,\lambda}^S + m_{ee,\lambda}^N|^2 + |m_{ee,\eta}^\nu + m_{ee,\eta}^S + m_{ee,\eta}^N|^2 \right] \quad (\text{B4})$$

Appendix C: A_4 group

A_4 is a group which represents even permutation of four objects. It has a total of 12 elements and have two generator, represented by S and T . A_4 has 4 conjugacy class which means that A_4 has four irreducible representation. Among those four irreducible representation, three are one dimensional ($1, 1', 1''$) and one is three dimensional. The product rules of two triplet (ψ_1, ψ_2, ψ_3) and (ϕ_1, ϕ_2, ϕ_3) in the T diagonal basis are given bellow

$$\begin{aligned} \begin{pmatrix} \psi_1 \\ \psi_2 \\ \psi_3 \end{pmatrix} \times \begin{pmatrix} \phi_1 \\ \phi_2 \\ \phi_3 \end{pmatrix} &= \begin{pmatrix} \psi_1\phi_1 + \psi_2\phi_3 + \psi_3\phi_2 \end{pmatrix} + \begin{pmatrix} \psi_3\phi_3 + \psi_1\phi_2 + \psi_2\phi_1 \end{pmatrix} + \begin{pmatrix} \psi_2\phi_2 + \psi_3\phi_1 + \psi_1\phi_3 \end{pmatrix} \\ &+ \begin{pmatrix} 2\psi_1\phi_1 - \psi_2\phi_3 - \psi_3\phi_2 \\ 2\psi_3\phi_3 - \psi_1\phi_2 - \psi_2\phi_1 \\ 2\psi_2\phi_2 - \psi_1\phi_3 - \psi_3\phi_1 \end{pmatrix} + \begin{pmatrix} \psi_2\phi_3 - \psi_3\phi_2 \\ \psi_1\phi_2 - \psi_2\phi_1 \\ \psi_3\phi_1 - \psi_1\phi_3 \end{pmatrix} . \end{aligned}$$

The multiplication rules are given bellow

$$3 \times 3 = 1 + 1' + 1'' + 3 + 3.$$

$$1' \times 1' = 1'', \quad 1' \times 1'' = 1, \quad 1'' \times 1'' = 1'.$$

-
- [1] S. Fukuda et al. Constraints on neutrino oscillations using 1258 days of Super-Kamiokande solar neutrino data. *Phys. Rev. Lett.*, 86:5656–5660, 2001.
 - [2] Q. R. Ahmad et al. Measurement of day and night neutrino energy spectra at SNO and constraints on neutrino mixing parameters. *Phys. Rev. Lett.*, 89:011302, 2002.
 - [3] Q. R. Ahmad et al. Direct evidence for neutrino flavor transformation from neutral current interactions in the Sudbury Neutrino Observatory. *Phys. Rev. Lett.*, 89:011301, 2002.
 - [4] Abhijit Bandyopadhyay, Sandhya Choubey, Srubabati Goswami, and Kamales Kar. Impact of the first SNO results on neutrino mass and mixing. *Phys. Lett. B*, 519:83–92, 2001.
 - [5] Justin Evans. The MINOS Experiment: Results and Prospects. *Adv. High Energy Phys.*, 2013:182537, 2013.
 - [6] F. P. An et al. Observation of electron-antineutrino disappearance at Daya Bay. *Phys. Rev. Lett.*, 108:171803, 2012.
 - [7] K. Abe et al. Indication of Electron Neutrino Appearance from an Accelerator-produced Off-axis Muon Neutrino Beam. *Phys. Rev. Lett.*, 107:041801, 2011.
 - [8] Thierry Lasserre, Guillaume Mention, Michel Cribier, Antoine Collin, Vincent Durand, Vincent Fischer, Jonathan Gaffiot, David Lhuillier, Alain Letourneau, and Matthieu Vivier. Comment on Phys. Rev. Lett. 108, 191802 (2012): ‘Observation of Reactor Electron Antineutrino Disappearance in the RENO Experiment’. 5 2012.
 - [9] N. Aghanim et al. Planck 2018 results. VI. Cosmological parameters. *Astron. Astrophys.*, 641:A6, 2020. [Erratum: *Astron.Astrophys.* 652, C4 (2021)].
 - [10] X. Qian and P. Vogel. Neutrino Mass Hierarchy. *Prog. Part. Nucl. Phys.*, 83:1–30, 2015.
 - [11] Anushree Ghosh, Tarak Thakore, and Sandhya Choubey. Determining the Neutrino Mass Hierarchy with INO, T2K, NOvA and Reactor Experiments. *JHEP*, 04:009, 2013.
 - [12] G. Barenboim, John F. Beacom, L. Borissov, and Boris Kayser. CPT Violation and the Nature of Neutrinos. *Phys. Lett. B*, 537:227–232, 2002.
 - [13] M. Czakon, J. Gluza, and M. Zralek. Nature of neutrinos in the light of present and future experiments. *Phys. Lett. B*, 465:211–218, 1999.

- [14] Rabindra N. Mohapatra and Goran Senjanovic. Neutrino Mass and Spontaneous Parity Nonconservation. *Phys. Rev. Lett.*, 44:912, 1980.
- [15] Murray Gell-Mann, Pierre Ramond, and Richard Slansky. Complex Spinors and Unified Theories. *Conf. Proc. C*, 790927:315–321, 1979.
- [16] J. Schechter and J. W. F. Valle. Neutrino Masses in $SU(2) \times U(1)$ Theories. *Phys. Rev. D*, 22:2227, 1980.
- [17] T. P. Cheng and Ling-Fong Li. Neutrino Masses, Mixings and Oscillations in $SU(2) \times U(1)$ Models of Electroweak Interactions. *Phys. Rev. D*, 22:2860, 1980.
- [18] C. Wetterich. Neutrino Masses and the Scale of B-L Violation. *Nucl. Phys. B*, 187:343–375, 1981.
- [19] M. Magg and C. Wetterich. Neutrino Mass Problem and Gauge Hierarchy. *Phys. Lett. B*, 94:61–64, 1980.
- [20] Robert Foot, H. Lew, X. G. He, and Girish C. Joshi. Seesaw Neutrino Masses Induced by a Triplet of Leptons. *Z. Phys. C*, 44:441, 1989.
- [21] Jogesh C. Pati and Abdus Salam. Lepton Number as the Fourth Color. *Phys. Rev. D*, 10:275–289, 1974. [Erratum: *Phys.Rev.D* 11, 703–703 (1975)].
- [22] G. Senjanovic and Rabindra N. Mohapatra. Exact Left-Right Symmetry and Spontaneous Violation of Parity. *Phys. Rev. D*, 12:1502, 1975.
- [23] N. G. Deshpande, J. F. Gunion, Boris Kayser, and Fredrick I. Olness. Left-right symmetric electroweak models with triplet Higgs. *Phys. Rev. D*, 44:837–858, 1991.
- [24] R. N. Mohapatra and Jogesh C. Pati. A Natural Left-Right Symmetry. *Phys. Rev. D*, 11:2558, 1975.
- [25] H. Georgi and S. L. Glashow. Unity of All Elementary Particle Forces. *Phys. Rev. Lett.*, 32:438–441, 1974.
- [26] Thomas G. Rizzo and Goran Senjanovic. Grand Unification and Parity Restoration at Low-Energies. 1. Phenomenology. *Phys. Rev. D*, 24:704, 1981. [Erratum: *Phys.Rev.D* 25, 1447 (1982)].
- [27] D. Chang, R. N. Mohapatra, and M. K. Parida. Decoupling Parity and $SU(2)$ -R Breaking Scales: A New Approach to Left-Right Symmetric Models. *Phys. Rev. Lett.*, 52:1072, 1984.
- [28] Stephen F. King and Christoph Luhn. Neutrino Mass and Mixing with Discrete Symmetry. *Rept. Prog. Phys.*, 76:056201, 2013.
- [29] Guido Altarelli and Ferruccio Feruglio. Discrete Flavor Symmetries and Models of Neutrino Mixing. *Rev. Mod. Phys.*, 82:2701–2729, 2010.
- [30] Ernest Ma and G. Rajasekaran. Softly broken $A(4)$ symmetry for nearly degenerate neutrino masses. *Phys. Rev. D*, 64:113012, 2001.
- [31] Guido Altarelli, Ferruccio Feruglio, and Luca Merlo. Revisiting Bimaximal Neutrino Mixing in a Model with $S(4)$ Discrete Symmetry. *JHEP*, 05:020, 2009.
- [32] Hajime Ishimori, Tatsuo Kobayashi, Hiroshi Ohki, Yusuke Shimizu, Hiroshi Okada, and Morimitsu Tanimoto. Non-Abelian Discrete Symmetries in Particle Physics. *Prog. Theor. Phys. Suppl.*, 183:1–163, 2010.

- [33] Tatsuo Kobayashi, Kentaro Tanaka, and Takuya H. Tatsuishi. Neutrino mixing from finite modular groups. *Phys. Rev. D*, 98(1):016004, 2018.
- [34] S. F. King. Unified Models of Neutrinos, Flavour and CP Violation. *Prog. Part. Nucl. Phys.*, 94:217–256, 2017.
- [35] P. P. Novichkov, J. T. Penedo, S. T. Petcov, and A. V. Titov. Generalised CP Symmetry in Modular-Invariant Models of Flavour. *JHEP*, 07:165, 2019.
- [36] Simon J. D. King and Stephen F. King. Fermion mass hierarchies from modular symmetry. *JHEP*, 09:043, 2020.
- [37] Reinier de Adelhart Toorop, Ferruccio Feruglio, and Claudia Hagedorn. Finite Modular Groups and Lepton Mixing. *Nucl. Phys. B*, 858:437–467, 2012.
- [38] Ferruccio Feruglio. *Are neutrino masses modular forms?*, pages 227–266. 2019.
- [39] Mitesh Kumar Behera, Subhasmita Mishra, Shivaramakrishna Singirala, and Rukmani Mohanta. Implications of A_4 modular symmetry on neutrino mass, mixing and leptogenesis with linear seesaw. *Phys. Dark Univ.*, 36:101027, 2022.
- [40] Takaaki Nomura, Hiroshi Okada, and Sudhanwa Patra. An inverse seesaw model with A_4 -modular symmetry. *Nucl. Phys. B*, 967:115395, 2021.
- [41] Jotin Gogoi, Nayana Gautam, and Mrinal Kumar Das. Neutrino masses and mixing in minimal inverse seesaw using A_4 modular symmetry. *Int. J. Mod. Phys. A*, 38(03):2350022, 2023.
- [42] Ranjeet Kumar, Priya Mishra, Mitesh Kumar Behera, Rukmani Mohanta, and Rahul Srivastava. Predictions from scoto-seesaw with A_4 modular symmetry. *Phys. Lett. B*, 853:138635, 2024.
- [43] Monal Kashav and Surender Verma. On minimal realization of topological Lorentz structures with one-loop seesaw extensions in A_4 modular symmetry. *JCAP*, 03:010, 2023.
- [44] Monal Kashav and Surender Verma. Broken scaling neutrino mass matrix and leptogenesis based on A_4 modular invariance. *JHEP*, 09:100, 2021.
- [45] Mitesh Kumar Behera, Shivaramakrishna Singirala, Subhasmita Mishra, and Rukmani Mohanta. A modular A_4 symmetric scotogenic model for neutrino mass and dark matter. *J. Phys. G*, 49(3):035002, 2022.
- [46] Francisco J. de Anda, Stephen F. King, and Elena Perdomo. $SU(5)$ grand unified theory with A_4 modular symmetry. *Phys. Rev. D*, 101(1):015028, 2020.
- [47] Hiroshi Okada and Yuta Orikasa. Neutrino mass model with a modular S_4 symmetry. 8 2019.
- [48] P. P. Novichkov, J. T. Penedo, and S. T. Petcov. Double cover of modular S_4 for flavour model building. *Nucl. Phys. B*, 963:115301, 2021.
- [49] J. T. Penedo and S. T. Petcov. Lepton Masses and Mixing from Modular S_4 Symmetry. *Nucl. Phys. B*, 939:292–307, 2019.

- [50] Gui-Jun Ding, Stephen F. King, and Chang-Yuan Yao. Modular $S_4 \times SU(5)$ GUT. *Phys. Rev. D*, 104(5):055034, 2021.
- [51] P. P. Novichkov, J. T. Penedo, S. T. Petcov, and A. V. Titov. Modular A_5 symmetry for flavour model building. *JHEP*, 04:174, 2019.
- [52] Bu-Yao Qu and Gui-Jun Ding. Non-holomorphic modular flavor symmetry. *JHEP*, 08:136, 2024.
- [53] Gui-Jun Ding, Ferruccio Feruglio, and Xiang-Gan Liu. Automorphic Forms and Fermion Masses. *JHEP*, 01:037, 2021.
- [54] D. Chang, R. N. Mohapatra, and M. K. Parida. A New Approach to Left-Right Symmetry Breaking in Unified Gauge Theories. *Phys. Rev. D*, 30:1052, 1984.
- [55] M. Sruthilaya, Rukmani Mohanta, and Sudhanwa Patra. Neutrino mass and neutrinoless double beta decay in $SO(10)$ GUT with Pati–Salam symmetry. *J. Phys. G*, 45(7):075004, 2018.
- [56] Francisco J. de Anda and Stephen F. King. Modular flavour symmetry and orbifolds. *JHEP*, 06:122, 2023.
- [57] S. Ferrara, . D. Lust, and S. Theisen. Target Space Modular Invariance and Low-Energy Couplings in Orbifold Compactifications. *Phys. Lett. B*, 233:147–152, 1989.
- [58] Gui-Jun Ding, Jun-Nan Lu, S. T. Petcov, and Bu-Yao Qu. Non-holomorphic Modular S_4 Lepton Flavour Models. 8 2024.
- [59] Supriya Senapati, Sudhanwa Patra, Prativa Pritimita, and Chayan Majumdar. A comparative study of $0\nu\beta\beta$ decay in symmetric and asymmetric left-right model. *Nucl. Phys. B*, 954:115000, 2020.
- [60] Ram Lal Awasthi, M. K. Parida, and Sudhanwa Patra. Neutrino masses, dominant neutrinoless double beta decay, and observable lepton flavor violation in left-right models and $SO(10)$ grand unification with low mass W_R, Z_R bosons. *JHEP*, 08:122, 2013.
- [61] M. K. Parida and Sudhanwa Patra. Left-right models with light neutrino mass prediction and dominant neutrinoless double beta decay rate. *Phys. Lett. B*, 718:1407–1412, 2013.
- [62] W. Grimus and L. Lavoura. The Seesaw mechanism at arbitrary order: Disentangling the small scale from the large scale. *JHEP*, 11:042, 2000.
- [63] Ivan Esteban, M. C. Gonzalez-Garcia, Michele Maltoni, Ivan Martinez-Soler, João Paulo Pinheiro, and Thomas Schwetz. NuFit-6.0: updated global analysis of three-flavor neutrino oscillations. *JHEP*, 12:216, 2024.
- [64] P. S. Bhupal Dev and R. N. Mohapatra. TeV Scale Inverse Seesaw in $SO(10)$ and Leptonic Non-Unitarity Effects. *Phys. Rev. D*, 81:013001, 2010.
- [65] Ram Lal Awasthi and Mina K. Parida. Inverse Seesaw Mechanism in Nonsupersymmetric $SO(10)$, Proton Lifetime, Nonunitarity Effects, and a Low-mass Z' Boson. *Phys. Rev. D*, 86:093004, 2012.
- [66] Enrique Fernandez-Martinez, Josu Hernandez-Garcia, and Jacobo Lopez-Pavon. Global constraints on heavy neutrino mixing. *JHEP*, 08:033, 2016.

- [67] Prativa Pritimita, Nitali Dash, and Sudhanwa Patra. Neutrinoless Double Beta Decay in LRSM with Natural Type-II seesaw Dominance. *JHEP*, 10:147, 2016.
- [68] Alberto Garfagnini. Latest results from GERDA Phase II experiment on ^{76}Ge double-beta decay and exotic decay searches. *PoS*, EPS-HEP2023:158, 2024.
- [69] G. Anton et al. Search for Neutrinoless Double- β Decay with the Complete EXO-200 Dataset. *Phys. Rev. Lett.*, 123(16):161802, 2019.
- [70] S. Abe et al. Search for the Majorana Nature of Neutrinos in the Inverted Mass Ordering Region with KamLAND-Zen. *Phys. Rev. Lett.*, 130(5):051801, 2023.
- [71] A. Gando et al. Limit on Neutrinoless $\beta\beta$ Decay of ^{136}Xe from the First Phase of KamLAND-Zen and Comparison with the Positive Claim in ^{76}Ge . *Phys. Rev. Lett.*, 110(6):062502, 2013.
- [72] James Barry and Werner Rodejohann. Lepton number and flavour violation in TeV-scale left-right symmetric theories with large left-right mixing. *JHEP*, 09:153, 2013.
- [73] K. Muto, E. Bender, and H. V. Klapdor. Nuclear Structure Effects on the Neutrinoless Double Beta Decay. *Z. Phys. A*, 334:187–194, 1989.